

NEUROMUSCULAR NEUTRAL ZONES RESPONSE TO
CYCLIC LUMBAR FLEXION

by
Deborah Solomonow

ARTHUR LAKES LIBRARY
COLORADO SCHOOL OF MINES
GOLDEN, CO. 80401

ProQuest Number: 10795109

All rights reserved

INFORMATION TO ALL USERS

The quality of this reproduction is dependent upon the quality of the copy submitted.

In the unlikely event that the author did not send a complete manuscript and there are missing pages, these will be noted. Also, if material had to be removed, a note will indicate the deletion.



ProQuest 10795109

Published by ProQuest LLC (2018). Copyright of the Dissertation is held by the Author.

All rights reserved.

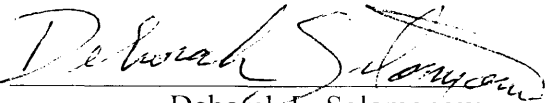
This work is protected against unauthorized copying under Title 17, United States Code
Microform Edition © ProQuest LLC.

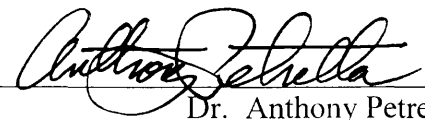
ProQuest LLC.
789 East Eisenhower Parkway
P.O. Box 1346
Ann Arbor, MI 48106 – 1346

A thesis submitted to the Faculty and the Board of Trustees of the Colorado School of Mines in partial fulfillment of the requirements for the degree of Master of Science (Engineering).

Golden, Colorado

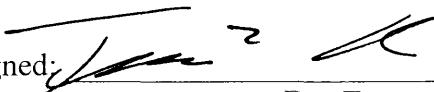
Date 4/2/2008

Signed: 
Debofah L. Solomonow

Signed: 
Dr. Anthony Petrella
Thesis Advisor

Golden, Colorado

Date 04/02/08

Signed: 
Dr. Terence Parker
Professor and Head
Division of Engineering

ABSTRACT

The response of the lumbar Neuromuscular Neutral Zones (NNZs) to 60 minutes of cumulative cyclic loading at 0.25Hz and 40N peak was assessed in the *in vivo* feline. Single-cycle tests were applied before the cyclic loading, and periodically during the 7-hour post-loading rest period. Lumbar displacement and tension of the supraspinous ligament, and electromyography (EMG) activity of the multifidus muscles were recorded throughout. Viscoelastic creep, displacement and tension NNZs increased significantly after loading indicating a substantial decrease in lumbar stability. The displacement NNZs decreased exponentially to near pre-loading value by the 7th hour of the post loading recovery period. The tension NNZs, however, decreased to below the pre-loading baseline by the 2nd to 3rd hour post loading and continued decreasing to the 7th hour. Peak EMG significantly decreased (49%-57%) to below the pre-loading baseline immediately after loading and then exponentially increased, exceeding the pre-loading baseline by the 2nd to 3rd hour, after which it further increased (33%-59%) above the baseline by the 7th hour. EMG median frequency followed a similar pattern to that of the peak EMG suggesting that normally active motor units were derecruited in the 2-3 hours after loading and re-recruited, together with new motor units, thereafter. Peak displacement (creep/laxity of the supraspinous ligament) accumulated throughout the loading session, and remained elevated until its exponential decrease reached the baseline by the 7th hour of recovery. These findings suggest that the lumbar spine was exposed to instability during the 2-3 hours immediately after loading due to concurrent laxity of the viscoelastic tissues and deficient muscular activity and force, thus increasing the risk of spinal injury. After 2-3 hours post cyclic loading, a neuromuscular compensation mechanism was found to exist, triggering the musculature significantly earlier and at higher magnitude than baseline, and recruiting additional normally inactive motor units, while the viscoelastic tissues were still lax. The findings above provide new insights on the effect of repetitive occupational activities on spinal stability and can be used for design of work schedules to prevent or attenuate the negative impact on workers in this category.

TABLE OF CONTENTS

ABSTRACT.....	iii
LIST OF FIGURES.....	vi
LIST OF TABLES.....	viii
ACKNOWLEDGEMENTS.....	ix
DEDICATION.....	x
CHAPTER 1 INTRODUCTION.....	1
1.1 Social, Clinical, and Epidemiological Relevance.....	1
1.2 Hypothesis.....	3
1.3 Significance of Study.....	3
CHAPTER 2 BACKGROUND.....	4
2.1 Anatomy of the Spinal Vertebrae and Joints, Spinal Viscoelastic Tissues, and Paraspinal Muscles.....	4
2.2 Spinal Stability and its Physiological Mechanisms.....	9
2.3 Histology of Viscoelastic Tissues.....	11
2.4 Creep of Viscoelastic Tissues.....	11
2.5 Electromyography (EMG) and its Measurement.....	13
2.6 EMG Amplitude, EMG Median Frequency, and Motor Unit Recruitment.....	14
CHAPTER 3 EXPERIMENTAL METHODS.....	16
3.1 Preparation.....	16
3.2 Instrumentation.....	16
3.3 Protocol.....	17
3.4 Data Processing.....	18
3.5 Statistics.....	20
3.6 Modeling.....	20
CHAPTER 4 RESULTS.....	24
4.1 Displacement Neuromuscular Neutral Zones (DNNZs).....	25
4.1.1 DNNZs in the Stretch Phase.....	26
4.1.2 DNNZs in the Release Phase.....	27

4.2 Tension Neuromuscular Neutral Zones (TNNZs).....	27
4.2.1 TNNZs in the Stretch Phase.....	29
4.2.2 TNNZs in the Release Phase.....	29
4.3 Normalized EMG Peak Mean Absolute Value (EPMAV).....	30
4.4 EMG Median Frequency (EMF).....	32
4.5 Creep Response.....	34
4.6 Modeling of DNNZ, TNNZ, EPMAV, and EMF Data.....	36
4.6.1 DNNZ Model.....	36
4.6.2 TNNZ Model.....	37
4.6.3 EPMAV Model.....	37
4.6.4 EMF Model.....	38
CHAPTER 5 DISCUSSION.....	40
5.1 Spinal Instability after Cyclic Loading.....	40
5.2 Compensatory Neural Mechanism.....	42
5.3 Statistical Analysis.....	43
5.4 Empirical Models.....	44
5.5 Comparison of Cyclic and Static Loading.....	45
5.6 Extrapolation/Applicability of Data from Feline Model to Human.....	47
CHAPTER 6 CONCLUSION.....	49
REFERENCES CITED.....	50

LIST OF FIGURES

Figure 2.1: Vertebrae of the spine. (NIH 2007).....	4
Figure 2.2: Lumbar vertebra from above and behind. (adapted from Gray’s Anatomy of the Human Body online edition, 2000, modified to enhance labels).....	5
Figure 2.3: (a) Posterior view of two vertebrae showing intervertebral disc and facet joints and capsules. (b) Side view of two vertebrae showing intervertebral discs, and depicting facet joint dynamics during flexion and extension. (adapted from http://www.spineuniverse.com/displayarticle.php/article1293.html).....	6
Figure 2.4: Median sagittal section of the vertebral column depicting ligaments of the spine. (adapted from Gray’s Anatomy of the Human Body online edition, 2000).....	6
Figure 2.5: Paraspinal muscles. (adapted from Gray’s Anatomy of the Human Body online edition, 2000).....	8
Figure 2.6: Feedback control system of the spine. (adapted from Solomonow et al, 2001).....	10
Figure 2.7: Displacement vs. Time and Load vs. Time plots depicting the scenario of development of creep in a viscoelastic material over some duration of application of a constant load (L_i and L_f are initial and final displacements, respectively).	12
Figure 2.8: Typical tension vs. displacement hysteresis curve from single passive stretch-release cycle applied to a feline supraspinous ligament.	13
Figure 2.9: Sample recording of a reflexive EMG signal from a feline multifidus muscle elicited by a single passive stretch-release cycle applied to a supraspinous ligament, the corresponding applied load and observed displacement, the NNZs duration indicated in red, and the corresponding DNNZ and TNNZ Thresholds indicated in green.	14
Figure 3.1: Loading sequence schematic and protocol parameters.	17
Figure 4.1: Typical recording of raw EMG from L3-4, L4-5, and L5-6, and corresponding tension and displacement vs. time during entire loading sequence.	24
Figure 4.2: Typical recording of EMG from L3-4, L4-5, and L5-6 with superimposed MAV and arrows indicating initiation and cessation NNZ thresholds, and corresponding tension and displacement vs. time during single loading cycle.	25
Figure 4.3: Mean \pm SD of DNNZ thresholds during stretch and release phases for data pooled across lumbar level vs. time with superimposed empirical models. Data points at time zero are baseline values from averaged pre – loading tests. Subsequent data is from recovery period.	25

Figure 4.4: Average percent difference from baseline values vs. time of DNNZ thresholds. Negative percent values represent below-baseline data. Lumbar levels are combined. * next to data points indicates statistically significant difference from baseline, as revealed by the post hoc Tukey HSD test. 26

Figure 4.5: Mean \pm SD of TNNZ thresholds during stretch and release phases for data pooled across lumbar level vs. time with superimposed empirical models. Data points at time zero are baseline values from averaged pre – loading tests. Subsequent data is from recovery period. 28

Figure 4.6: Average percent difference from baseline vs. time of TNNZ thresholds. Negative percent values represent below-baseline data. Lumbar levels are combined. * next to data points indicates statistically significant difference from baseline, as revealed by the post hoc Tukey HSD test. 28

Figure 4.7: Mean \pm SD of EPMAV for data pooled across lumbar level vs. time with superimposed empirical models. Data pts. at time zero are baseline values from avg'd pre – loading tests. Subsequent data is from recovery period... 30

Figure 4.8: Average percent difference from baseline vs. time of EPMAV. Negative percent values represent below-baseline data. Lumbar levels are combined. * next to data points indicates statistically significant difference from baseline, as revealed by the post hoc Tukey HSD test. 31

Figure 4.9: Mean \pm SD of EMF for data pooled across lumbar level vs. time. Data points at time zero are baseline value from averaged pre – loading tests. Subsequent data is from recovery period. 32

Figure 4.10: Mean \pm SD of EMF, smoothed with a 3-point moving average algorithm, for data pooled across lumbar level vs. time with superimposed empirical models. Data points at time zero are baseline values from averaged pre – loading tests. Subsequent data is from recovery period. 32

Figure 4.11: Average percent difference from baseline vs. time of EMF. Negative percent values represent below-baseline data. Lumbar levels are combined. * next to data points indicates statistically significant difference from baseline, as revealed by the post hoc Tukey HSD test. 33

Figure 4.12: Mean \pm SD of peak displacement vs. time from beginning of loading until end of recovery. Only values from first and last cycle of each loading block are shown, as well as peak displacement for all single-cycle tests during recovery. On time axis, eob=end of block and bob=beginning of block. 35

Figure 4.13: Average percent difference, of each peak displacement measurement for each feline preparation and all lumbar levels, from the first peak displacement measurement at time bob 1. Only values from first and last cycle of each loading block are shown, as well as for all single-cycle tests during recovery. On time axis, eob=end of block and bob=beginning of block. 35

LIST OF TABLES

Table 3.1: Definition/description of coefficients and terms of DNNZ(t).	21
Table 3.2: Definition/description of coefficients and terms of TNNZ(t).	21
Table 3.3: Definition/description of coefficients and terms of EPMAV(t).	22
Table 3.4: Definition/description of coefficients and terms of EMF(t).	23
Table 4.1: DNNZ empirical model coefficient and time constant values and regression coefficients for stretch and release phases of each lumbar level obtained by Levenberg-Marquart nonlinear regression algorithms.	36
Table 4.2: TNNZ empirical model coefficient and time constant values and regression coefficients for stretch and release phases of each lumbar level obtained by Levenberg-Marquart nonlinear regression algorithms.	37
Table 4.3: EPMAV empirical model coefficient and time constant values and regression coefficients for each lumbar level obtained by Levenberg-Marquart nonlinear regression algorithms.	38
Table 4.4: EMF empirical model coefficient and time constant values and regression coefficients for each lumbar level obtained by Levenberg-Marquart nonlinear regression algorithms.	39

ACKNOWLEDGEMENTS

I thank God, with Whom all things are possible, and without Whom this work would not be.

I thank my father and research advisor, Dr. Moshe Solomonow. He has taught me valuable lessons in both life and academics. He has challenged me to work hard, even in times of intellectual exhaustion, and given me tools to be successful. I also thank my mother who has supported me throughout my life, and in times of stress during my educational career post Hurricane Katrina. Thank you Mom and Dad! I thank my grandparents for always praying for me to be happy and successful in life, and for being proud of me when I am. Thank you Saba and Safta!

I thank Dr. Yun Lu and Dr. Bing He Zhou, who are like family to me. Thank you for helping me with everything and believing in me throughout my life.

I thank my committee, Dr. Anthony Petrella and Dr. Tyrone Vincent, for answering my questions and for taking time to review my thesis and participate in my defense. I also thank Dr. Joel Bach for his support and for recommending me for teaching assistantships. I thank Dr. Brad Davidson for taking time to answer my many question and teach me how to use statistics, empirical modeling, and all things involved in graduate research in general.

Finally, I would like to thank Dr. Russell Trahan and Dr. Vesselin Jilkov from the University of New Orleans for supporting me through the most challenging semester immediately post Hurricane Katrina. I wish you and UNO full recovery to the pre-Katrina glory.

To my dear grandparents, Yonatan and Chava Solomonow,
and my parents, Dr. Moshe and Susanne Solomonow.

CHAPTER 1

INTRODUCTION

Low back pain, disorders, and injury are a major problem in the world today, having many social and clinical implications. Studies have confirmed various types of cyclic loading that are detrimental to one's health in many ways and have identified several mechanisms relating to these detrimental consequences. This study aims to better understand the mechanisms and consequences related to this type of loading. This chapter describes the relevance and significance of this study according to several epidemiological statistics and many previous studies, as well as the hypothesized outcome.

1.1 **Social, Clinical, and Epidemiological Relevance**

Low back injury, pain, and disorders are associated with many repetitive (cyclic) occupational activities, and are a significant international problem, affecting a large number of the population, and costing a substantial amount of money every year (Hoogendoorn et al. 2000; Marras 2000; Panjabi 1996; Punnett and Wegman 2004; Silverstein and Clark 2004). In 2004, the leading cause of missed workdays was injuries of the low back (Bureau of Labor Statistics). Individuals and corporations lose over an estimated \$10 billion per year just in treating these injuries (NIOSH, 1999). In addition, 65 to 80 % of Americans will experience low back pain sometime in their lives (Manchikanti 2000).

Workers subjected to cyclic and static activities were shown to have many more incidences of low back disorders compared to the general population (Andersson 1981; Marras et al. 1995; Marras et al. 1993; McGill 1997; Punnett et al. 1991; Xu et al. 1997). Cyclic/repetitive sports and occupational activities were shown to trigger high rates of musculoskeletal disorders when performed over long periods (Hoogendoorn et al. 2000; Marras 2000; Silverstein et al. 1986). Biological and histological evidence has not been available until recently. The above epidemiology was recently confirmed biomechanically and physiologically in *in vivo* animal models (Hoops et al. 2007; Le et al. 2007; Navar et al. 2006) and in humans (Dickey et al. 2003; Granata et al. 2005;

Karajcarski 2006; Li et al. 2007; Olson et al. 2006; Olson et al. 2004; 2007; Shin and Mirka 2007). Prolonged periods of exposure to cyclic lumbar loading were shown to develop substantial laxity/creep in the viscoelastic tissues and in turn, significant changes in the activation pattern of the spinal musculature (Dickey et al. 2003; Li et al. 2007; Olson et al. 2004; Solomonow et al. 2001; van Dieen et al. 2003). A neuromuscular disorder consisting of spasms and temporary attenuation of muscle activity, followed by hyperexcitability was observed to be associated with excessive cyclic loading (Hoops et al. 2007; Le et al. 2007; Navar et al. 2006).

It is expected that cyclic activity of the lumbar spine may also elicit pronounced changes in the NNZs and elicit pronounced changes in spinal stability. Studies have suggested that spinal instability can lead to or be the cause of low back pain (Omino and Hayashi 1992; Panjabi 1996; Preuss and Fung 2005). In addition, cyclic load duration, short rest periods between cyclic loading, cyclic loading rate, high-repetition cyclic loading, and cyclic load magnitude have all been shown to be risk factors for the development of an acute neuromuscular disorder, creep, and spinal instability (Eversull et al. 2001; Gedalia et al. 1999; Hoops et al. 2007; Le et al. 2007; Lu et al. 2004; Navar et al. 2006; Sbriccoli et al. 2004a; Sbriccoli et al. 2004b; Solomonow et al. 1999).

One specific disorder resulting from cyclic activities is known as Cumulative Trauma Disorder (CTD), or Cumulative Low Back Disorder (CLBD), characterized by pain, weakness, limited range of motion, stiffness, and spasms of the back muscles (Courville et al. 2005; LaBry et al. 2004; Sbriccoli et al. 2004b). Risk factors of CTD include those discussed above (load duration, short rest periods, loading rate, number of repetitions, and load magnitude). In addition, workers subjected to cyclic, static, and vibratory loading for extended periods of time are at risk for developing CTD (Hoogendoorn et al. 2000; Punnett et al. 1991; Silverstein et al. 1986). CTD is a chronic disorder that does not generally improve with medical therapies (Courville et al. 2005) and cannot be confirmed by diagnostic procedures (LaBry et al. 2004). In cyclic loading, creep has been shown to accumulate over loading time, and does not recover in the same amount of time that it takes to induce the creep (Crisco et al. 1997; Ekstrom et al. 1996; Gedalia et al. 1999; Solomonow et al. 2003b). If there are insufficient rest periods between loading durations, and loading activities are performed daily, creep will continue

to accumulate over months and years until it becomes a chronic disorder as described above.

1.2 **Hypothesis**

We hypothesize that 60 minutes of cyclic lumbar loading at a moderate load will create creep in the viscoelastic tissues, cause significant enlargement of the NNZs immediately after loading, and that several hours of rest will be required to restore normal viscoelastic tissue properties and NNZs. The enlargement of NNZs would indicate reduction in spinal stability, as stabilizing reflexive muscular activity will initiate and cease at larger displacements and loads of the viscoelastic tissues, leaving a larger range at the beginning and end of each stretch-release cycle in which the spine is not protected or stiffened by the musculature. We further predict that pronounced changes may be observed in the EMG amplitude and EMG median frequency when comparing it before and after cyclic loading.

1.3 **Significance of Study**

The new information from this study can afford new insights into the changes in the motor control responsible for the stability of the lumbar spine after cyclic work, the potential for injury and the development of a means for its prevention, as well as prevention of neuromuscular disorders such as CTD, and baseline data for design of safe work scheduling. From the systems engineering standpoint, it will provide data that can characterize the ligamento-muscular feedback loop that governs spinal stability. Future studies will be needed to find a transformation to extrapolate the data obtained for the feline model of this study to a human model in order to design the safe working conditions.

CHAPTER 2 BACKGROUND

There are several major fundamental understandings necessary for the full appreciation of the information used and obtained in this study. Among them are the anatomy of the spinal vertebrae and joints, spinal viscoelastic tissues, and paraspinal muscles, the concept of spinal stability and the physiological mechanisms that govern it, histology and creep of viscoelastic tissues, EMG and its measurement, and EMG amplitude, median frequency, and their relationship to motor unit recruitment. This chapter gives an overview of the above-mentioned background information.

2.1 Anatomy of the Spinal Vertebrae and Joints, Spinal Viscoelastic Tissues, and Paraspinal Muscles

The anatomical structures relevant to this study include the spinal vertebrae and joints, spinal viscoelastic tissues, and paraspinal muscles.

The spine itself consists of several levels of vertebrae as shown in Figure 2.1.

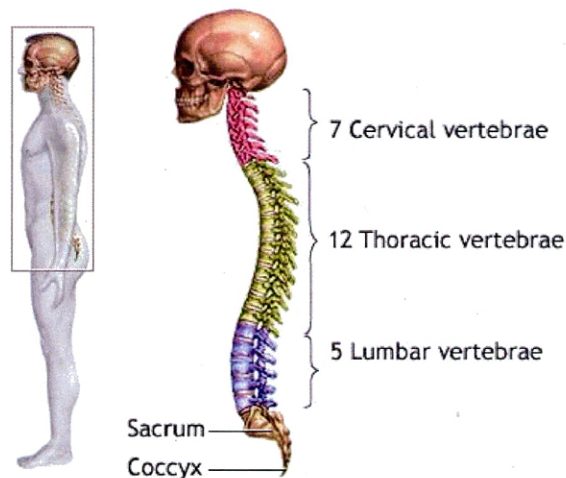


Figure 2.1: Vertebrae of the spine. (NIH 2007)

The vertebrae, stacked one on top of the other, extend from the base of skull to the tailbone. Each level of the spine (cervical, thoracic, lumbar, sacrum, and coccyx) contains a different number of vertebrae, as seen in the figure. The relatively flexible cervical vertebrae are located in the neck, and support the weight of the head, allowing

sagittal and lateral flexion-extension, and axial rotation. The thoracic vertebrae, which compose the upper back, are relatively inflexible, as they are attached to the rib cage at each level. They support and provide stability for the upper body. The lumbar vertebrae, located in the lower back carry the weight of the upper body, and are relatively flexible, allowing motion such as sagittal flexion-extension, lateral extension, and axial rotation. Most of the movement occurs in this region, relative to other regions, in flexion activities. This lower back lumbar region of the spine, due to its above-mentioned characteristics, is of specific interest in this study, as it is especially susceptible to injury, pain, and disorders. The sacrum consists of five vertebrae fused together to form a triangular bone that joins the spine with the pelvis. The coccyx consists of four fused vertebrae and is referred to as the tailbone. The sacrum and coccyx do not allow movement.

Figure 2.2 shows an individual lumbar vertebra, in which the posterior spinous process can be seen at the far top, along with the several processes on either side.

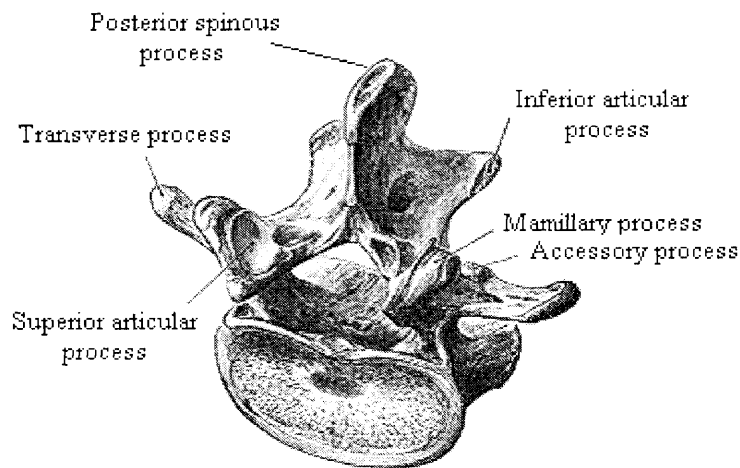


Figure 2.2: Lumbar vertebra from above and behind. (adapted from Gray's Anatomy of the Human Body online edition, 2000, modified to enhance labels)

The grooves on either side of the spinous processes serve as a junction for the spine to be connected to the paraspinal muscles, described later in this section.

Each vertebra has two paired facet joints located on either side of the spinous process, as seen in Figure 2.3(a). These small joints interlock with adjacent vertebrae on the top and bottom of each vertebra, and aid in stability, limiting rotation and sliding of one vertebra relative to another. Figure 2.3(b) depicts the facet joint dynamics during flexion and extension.

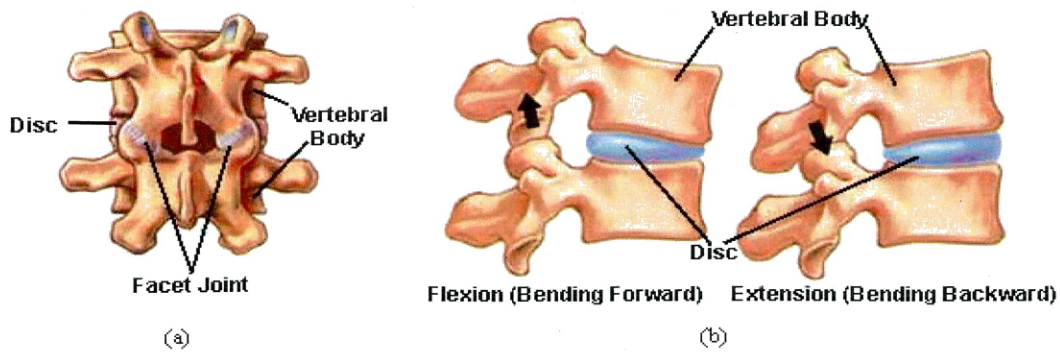


Figure 2.3: (a) Posterior view of two vertebrae showing intervertebral disc and facet joints and capsules. (b) Side view of two vertebrae showing intervertebral discs, and depicting facet joint dynamics during flexion and extension. (adapted from <http://www.spineuniverse.com/displayarticle.php/article1293.html>)

The major viscoelastic tissues of the spine consist of spinal ligaments, discs, and facet capsules, among others.

Fibrous cords or sheets called spinal ligaments, depicted in Figure 2.4, provide structural stability to the spine by holding vertebra together and providing resistance to excessive movement.

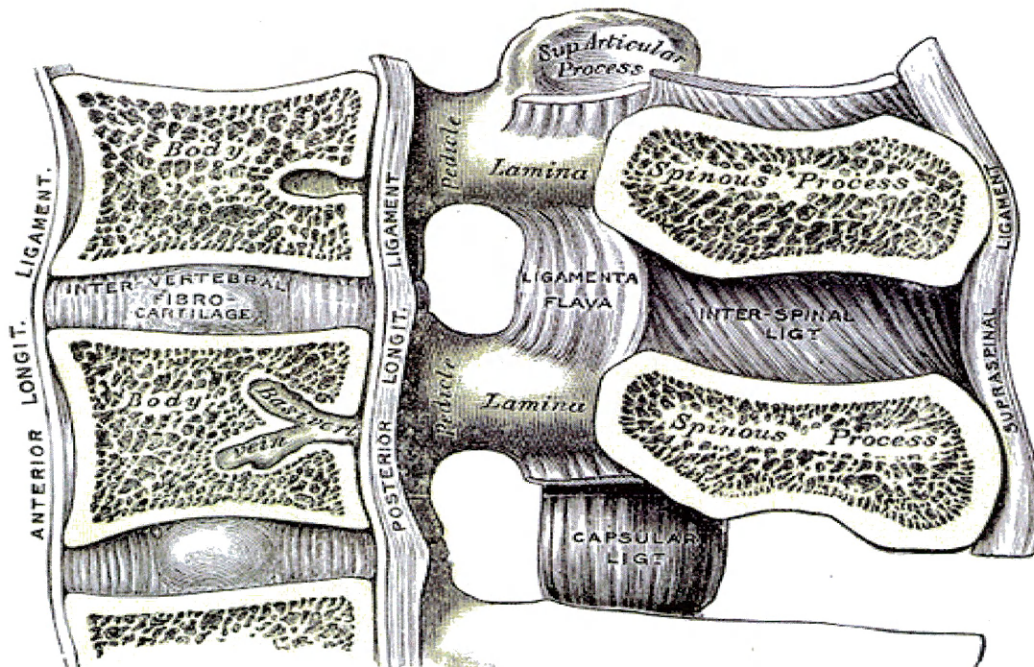


Figure 2.4: Median sagittal section of the vertebral column depicting ligaments of the spine. (adapted from Gray's Anatomy of the Human Body online edition, 2000)

They are composed of bundled collagen fibers and are more elastic than viscous in nature. The spine has numerous ligaments that connect individual vertebrae, or groups of vertebrae. Of specific interest in this study is the supraspinous ligament, a strong fibrous cord seen in the far right of Figure 2.4, that connects the tips of the posterior spinous processes of the vertebrae from the seventh cervical vertebra to the sacrum.

Each adjacent vertebra of the spine is separated by intervertebral discs, which connect vertebrae together, act as cushions between adjacent vertebrae, and function as shock absorbers. They are more viscous than elastic in nature, and are composed of fluid surrounded by a fibrous collagen membrane. The discs also provide stability in the form of stiffness and resistance to excessive motion of one vertebra relative to another, while also allowing some flexibility. They can be seen in Figure 2.3.

Facet capsules are made up of collagenous membranes that surround and enclose each facet joint. They are depicted in Figure 2.3(a) in white at the facet joints. They provide resistance to excessive motion.

Paraspinal muscles are the posterior muscles next to the spine. They provide stability, maintain posture, and generate movement. There are numerous types of these muscles; however, of specific interest in this study are the multifidus muscles, which fill up the grooves on both sides of the spinous processes. The multifidi, along with several other paraspinal muscles, can be seen in Figure 2.5. In the figure, the multifidi are shown to the immediate left of the posterior spinous processes, although the multifidus muscles are located on both the left and right in reality. The multifidus muscles are the deep back muscles that originate from the last four cervical vertebrae, the thoracic vertebrae, the lumbar vertebrae, and the sacrum. These muscles connect one vertebra to a vertebrae two to four levels below it. The multifidi are the closest muscles to the vertebrae with the shortest lever arm and low torque generating ability, thus being the major intervertebral stabilizing muscles. When they contract, they provide intervertebral stiffness.

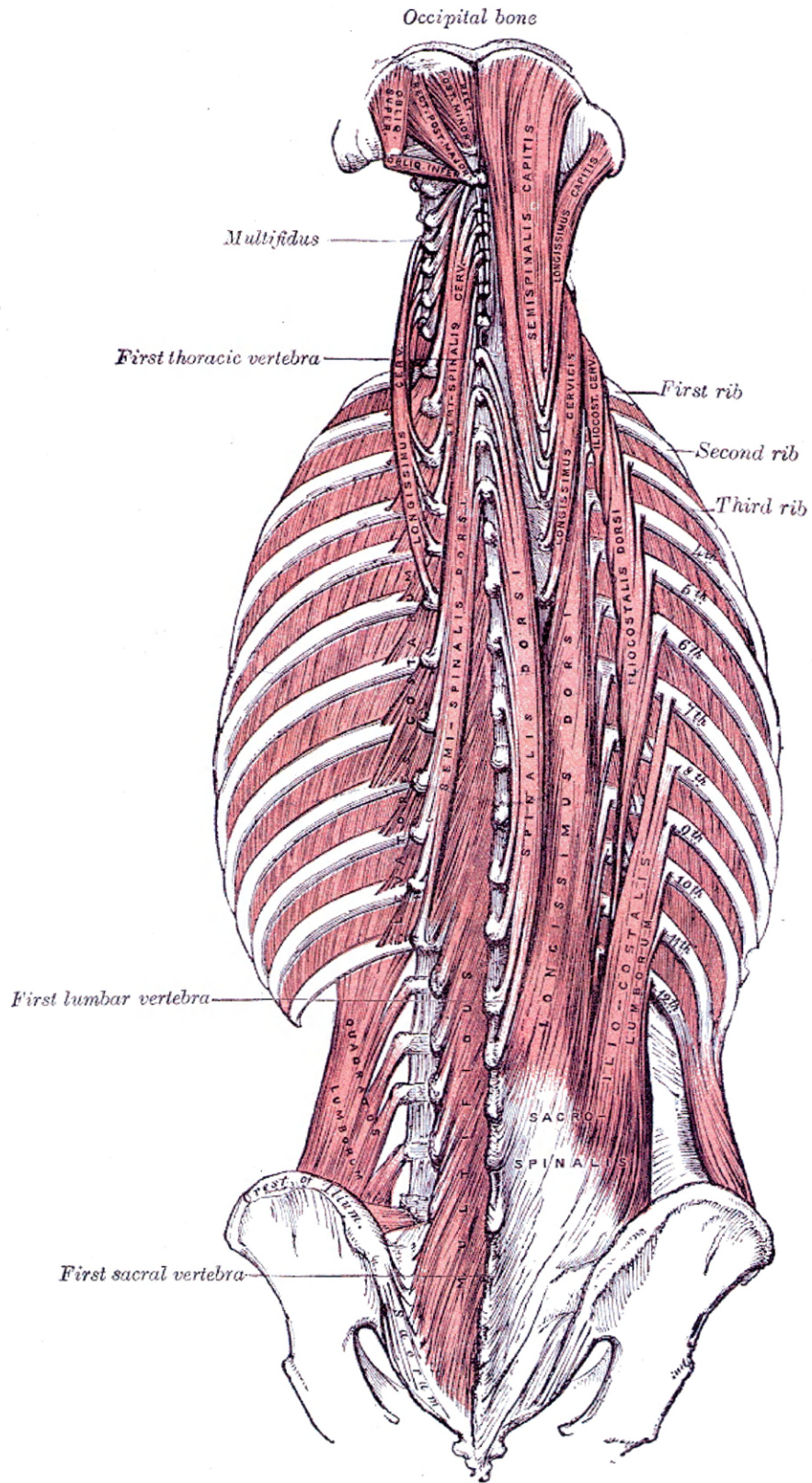


Figure 2.5: Paraspinal muscles. (adapted from Gray's Anatomy of the Human Body online edition, 2000)

2.2 Spinal Stability and its Physiological Mechanisms

A previous analysis (Reeves et al. 2007) defined spinal stability qualitatively. It suggested that a dynamically stable spine should allow the spine to bear loads, allow movement, and avoid injury and pain. In order to do so, it should return to its original behavior, if perturbed, with vertebrae staying within the vicinity of or returning to their intended unperturbed trajectories. It should also have the ability to limit the region in which the system lies by limiting the perturbation. This definition implies that a dynamically stable spine should not have excessive intervertebral motion in response to a perturbation, and that a relatively small perturbation should not cause excessive intervertebral motion, as this excessive motion could lead to injury.

The passive anatomical structures of the spine responsible for stability are the viscoelastic tissues (ligaments, discs, facet capsules, etc.), while the active tissues are the muscles. The muscles are, by far, the main structures responsible for dynamic stability relative to the viscoelastic tissues (Lucas et al. 1961; Panjabi 1992).

One component of structural stability of the intervertebral joints is the effect of the viscoelastic properties of the ligaments, discs, and facet capsules, among others. When vertebrae are displaced relative to each other, the various viscoelastic tissues deform and generate tension expressed as resistance to destabilizing motion. The passive resistance of the viscoelastic tissues is minimal for small perturbations about the neutral position and sharply increases for larger displacements. The ranges of small perturbation where the viscoelastic tissues are minimally engaged have been designated as Neutral Zones (NZs), within which, under normal conditions, the spine is inherently stable (Panjabi 1992; 1996).

Another important component of spine stability is the contribution of the muscles and their motor control (Adams 2007; Panjabi 1996). Muscles can be described as acting as guy wires in stabilizing the spine (Panjabi 1996). They also provide baseline muscle tone that maintains upright posture.

The active and passive components of spinal stability give rise to the motor control closed loop feedback system, depicted schematically in Figure 2.6, which links the stabilizing contributions of the active and passive tissues.

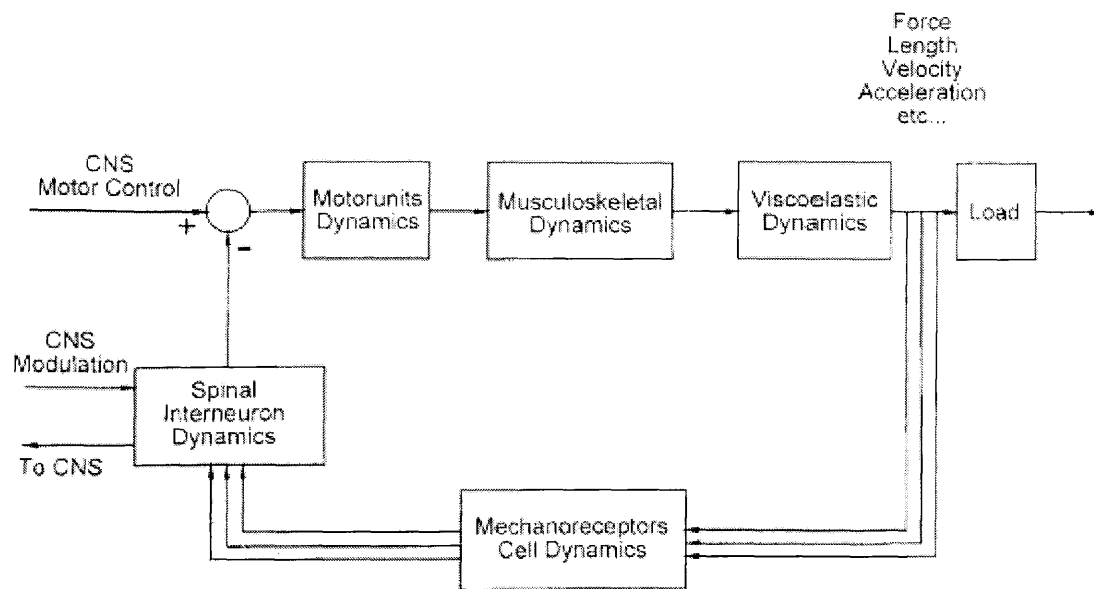


Figure 2.6: Feedback control system of the spine. (adapted from Solomonow et al, 2001)

The figure is a simplified diagram of a complex sensorimotor control system of the spine (Solomonow et al. 2003b; Solomonow et al. 2001). In essence, it depicts the load-sharing dynamics of several components of the spine stabilizing system, including motor unit, musculoskeletal, and viscoelastic dynamics, acting to control the force, length, velocity, acceleration, etc. of internal and external spinal loads. Mechanoreceptor feedback from several sources, including ligaments, discs, and facet capsules, is employed to optimally maintain spinal stability in carrying the load. Inputs to the forward segment come from the brain's motor control center via the Central Nervous System (CNS). Communication of the mechanoreceptors with the forward segment of the control system and the CNS occurs through interconnected neurons in the spinal tracts.

It is important to isolate one closed loop feedback system that exists within the complex control system depicted, called the ligamento-muscular protective reflex of the spine, as this reflex is of primary concern in this study. This reflex uses the sensory receptors (mechanoreceptors), described in Section 2.3, in the viscoelastic tissues of joints to monitor the level of stress or strain and transmit neural signals to the CNS that cause muscles to contract, thus stabilizing the joint (Baratta et al. 1988; Hirokawa 1991; Hirokawa et al. 1992; Solomonow et al. 1998; Stubbs et al. 1998). This study is concerned with the changes in the ligamento-muscular reflex under cyclic loading, and

the associated Neuromuscular Neutral Zones (NNZs). Recently, two studies (Eversull et al. 2001; Solomonow et al. 2001) described the NNZ thresholds, where passive intervertebral motion above a certain displacement, or a load above a certain magnitude, triggers the reflexive activation of the musculature to preserve stability (Stubbs et al. 1998).

It is necessary to note that although the stabilizing properties of the paraspinal muscles are of specific interest in this study, they are not the only muscles which contribute to stability. The agonist-antagonist relationship of paraspinal and abdominal muscles, for example, plays a critical role in maintaining spinal stability during active flexion-extension exercises. Abdominal muscles, such as the external and internal obliques and transversus, increase abdominal pressure, which in turn provides anterior spine stability. However, since passive loading is applied in this study, this agonist-antagonist relationship and the stabilizing properties of the abdominal and other muscles are not considered.

2.3 **Histology of Viscoelastic Tissues**

The mechanism of viscoelastic tissues to trigger reflexive muscular activity can be observed on a microscopic level. Viscoelastic tissues contain neural sensory receptors called mechanoreceptors that include Golgi, Ruffini, Pacinian, and bare nerve endings. Upon deformation of viscoelastic tissues (applying load or stretching), mechanoreceptors initiate action potentials which reflexively trigger muscle activation via the spinal mono- or oligo-synaptic connections of the receptor on the muscle's motor neurons. This reflex is known as the ligamento-muscular reflex, as stated in Section 2.2. With respect to stability of the spine, movement beyond the above-mentioned NNZs causes viscoelastic tissues to stretch to a point at which the ligamento-muscular reflex is employed.

2.4 **Creep of Viscoelastic Tissues**

Due to their viscoelastic properties, ligaments, discs, and facet capsules exhibit creep upon application of load. Applying a load to a viscoelastic material causes it to exhibit initial elongation and continue to elongate over time. Upon removing the load, the viscoelastic material does not immediately return to its original length, and may

require a substantial amount of time to do so. In fact, it has been shown to recover gradually in an exponential manner (Courville et al. 2005; Hoops et al. 2007; Le et al. 2007; Solomonow et al. 2003b). Creep can be defined as the percent change between displacement of a viscoelastic material at the onset of application of a constant load, and displacement after some duration of load application as

$$creep = \frac{L_f - L_i}{L_i} * 100,$$

where L_i and L_f are the initial and final displacements, respectively. Figure 2.7 depicts the scenario of the development of creep in a viscoelastic material over some duration of application of a constant load, and the beginning of its recovery after removal of the load, showing a Displacement vs. Time and corresponding Load vs. Time plot.

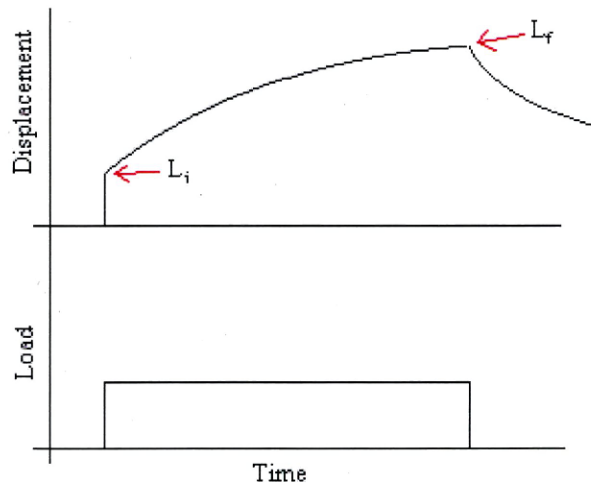


Figure 2.7: Displacement vs. Time and Load vs. Time plots depicting the scenario of development of creep in a viscoelastic material over some duration of application of a constant load. (L_i and L_f are initial and final displacements, respectively.)

Figure 2.8 shows a typical tension vs. displacement response, known as hysteresis, of the feline supraspinous ligament to a single passive cycle of stretch-release (flexion-extension).

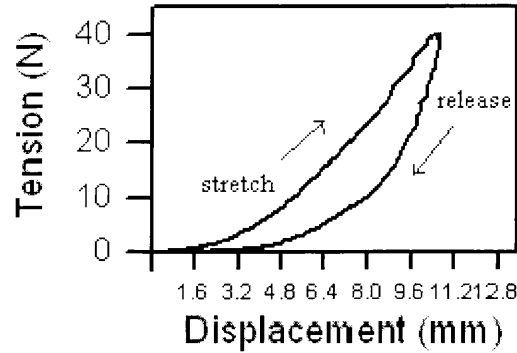


Figure 2.8: Typical tension vs. displacement hysteresis curve from single passive stretch-release cycle applied to a feline supraspinous ligament.

It can be seen from the figure that at a specific displacement, the tension value in the stretch phase is higher than that in the release phase, which indicates that creep was induced in the ligament.

2.5 Electromyography (EMG) and its Measurement

The recording of electrical muscle activity is called electromyography (EMG). When skeletal muscles are at rest, the muscle fibers composing them have a very small resting membrane potential. Muscles contract when motor neurons fire action potentials along muscle fibers. These action potentials vary in frequency.

The spatio-temporal summation of EMG action potentials can be picked up using a variety of EMG electrodes. For example, surface electrodes placed on the skin over a muscle fiber, in the direction of action potential conduction, pick up action potentials from many superficial muscles. In this study, fine wire electrode pairs inserted into the muscle were used, as they are capable of picking up the summation of action potentials from deep muscles, without cross talk from superficial muscles.

Because of their very small amplitude (mV range), and in order to filter unwanted environmental noise, EMG signals are usually differentially amplified. A bandpass filter, with pass band of 20 to 500 Hz, was applied to the EMG signals in this study. Frequencies lower than 20 Hz are attenuated in order to filter unwanted movement artifacts, and frequencies higher than 500 Hz are attenuated, as 95 % of EMG power from the multifidi exists below this frequency (Hoops et al. 2007). Figure 2.9 shows a sample

recording of a reflexive EMG signal from a feline multifidus muscle elicited by a single passive stretch-release cycle applied to a supraspinous ligament, the corresponding applied load and observed displacement, and the Neuromuscular Neutral Zones duration are indicated in red. The corresponding Displacement and Tension Neuromuscular Neutral Zone (DNNZ and TNNZ, respectively) thresholds are also shown in green.

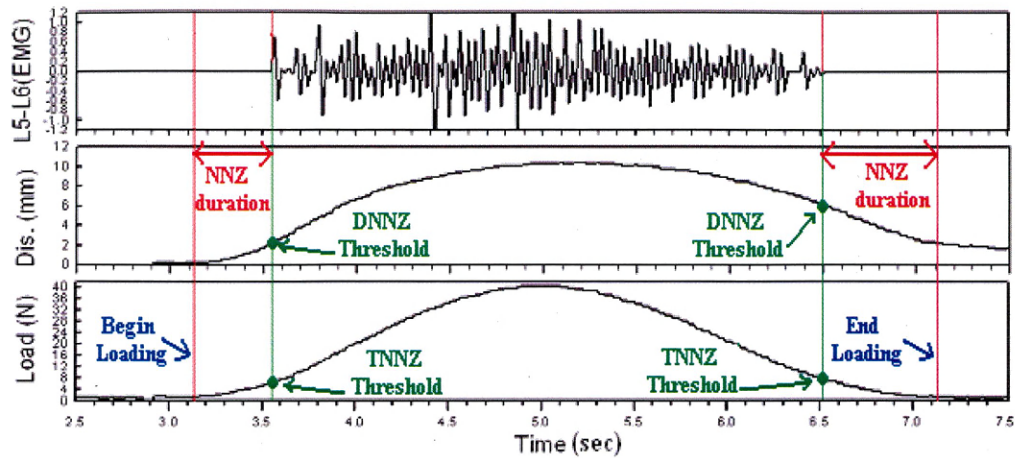


Figure 2.9: Sample recording of a reflexive EMG signal from a feline multifidus muscle elicited by a single passive stretch-release cycle applied to a supraspinous ligament, the corresponding applied load and observed displacement, the NNZs duration indicated in red, and the corresponding DNNZ and TNNZ thresholds indicated in green.

2.6 EMG Amplitude, EMG Median Frequency, and Motor Unit Recruitment

The response of EMG amplitude (absolute value of EMG) and EMG Median Frequency –EMF (defined as the frequency that divides the EMG power spectrum in half) is vital in providing a picture of changes in muscular activity and motor unit recruitment due to different loading conditions.

All muscles consist of motor units ranging in size. Some muscles have relatively larger motor units and some smaller. Those with predominantly larger motor units are known as fast twitch muscles, and have a relatively higher conduction velocity of action potentials. In this study, we are concerned with the lumbar multifidi, which are slow twitch muscles containing predominantly smaller motor units, and having a relatively lower conduction velocity of action potentials. The motor unit pool of the lumbar multifidi also ranges in size. When voluntarily or reflexively contracting a muscle, motor

units are recruited from smallest to largest as the need for more muscle force arises, in a process called orderly recruitment.

EMG frequencies are related to average conduction velocity of active motor units (Bellemere 1979; Givens and Teeple 1978; Kadefors et al. 1968; Lindstrom et al. 1970; Magora et al. 1976; Solomonow et al. 1990; Stulen and DeLuca 1981). In the absence of muscle fatigue, EMG amplitude is related to EMF, which is related to conduction velocity (CV). As the need for force increases, for example, the EMG amplitude increases and the EMF increases. In the presence of muscle fatigue, EMG amplitude increases, but the EMF decreases. The decrease in EMF, and thus CV, reflects overworked larger motor units dropping out of the active motor unit pool, in a process called orderly derecruitment. The increase in EMG amplitude, in this case, is caused by changes in the firing rate of smaller motor units, which in turn causes the amplitude of the spatio-temporal summation of action potentials to increase.

In this study, it was expected that muscle fatigue would not be present, as the level of activation from the passive cyclic loading was relatively low. This was indeed the case, as will be seen in the results chapter by the similar behavior of the EMG amplitude and EMF.

Calculations of EMF assume that the EMG is a stationary signal, which it is not. To circumvent this issue, only short time segments of the EMG are taken for calculations of EMF, with the assumption that the signal is stationary within that time period.

CHAPTER 3

EXPERIMENTAL METHODS

The following sections of this chapter describe the preparation of feline subjects used in this study, instrumentation used to collect relevant data, the protocol used in this experiment, data processing necessary to calculate and obtain necessary information from raw data, statistical analysis used to support conclusions from the experiment, and empirical modeling of resultant phenomena.

3.1 Preparation

Seven adult feline subjects (weight: 3.95 ± 0.37 kg), anesthetized with 60 mg/kg alpha-chloralose, were used in this study in accordance with a protocol approved by the Institutional Animal Care and Use Committee. An incision was made on the skin overlying the lumbar spine to expose the dorso-lumbar fascia. An S-shaped stainless steel hook (1.5-mm diameter rod) was inserted around the ligament between the L4 and L5 lumbar level vertebrae. The preparation was positioned in a rigid stainless steel frame and two external fixators attached to the frame were applied to the L1 and L7 posterior spinal processes in order to isolate the lumbar spine. These fixators were used to limit interaction of motion between the lumbar spine and thoracic, sacral, and pelvic structures.

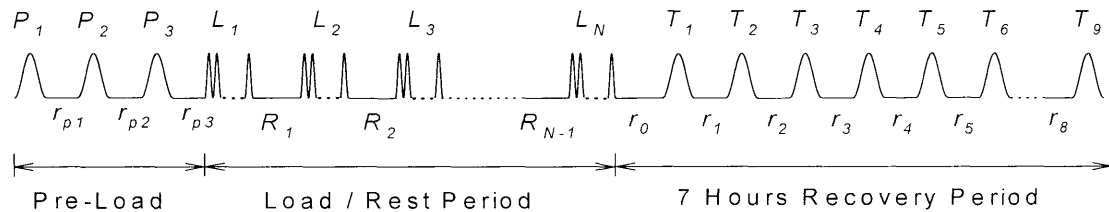
3.2 Instrumentation

Three pairs of stainless steel fine wire electrodes were inserted into the right L3-4, L4-5, and L5-6 multifidus muscle 6-8 mm lateral to the spinal processes with 3-4 mm interelectrode distance. A ground electrode was inserted into the gluteus muscle. Each pair of electrodes constituted an input into a differential electromyography (EMG) amplifier with a 110-dB common mode rejection ratio, gain of 500, and a bandpass filter in the range of 20-500 Hz. The free end of the S-shaped hook was connected to the vertical load actuator of the Bionix 858 Material Testing System (MTS, Minneapolis, MN). The load was applied via the actuator with a computer-controlled loading system. The EMG was sampled at 1,000 Hz, along with the vertical displacement and tension applied to the S-shaped hook, before storage on a computer. EMG was monitored

continuously on an oscilloscope and the applied tension and displacement were monitored continuously on the MTS computer screen.

3.3 Protocol

Single-cycle tests and blocks of cyclic loading were applied sinusoidally at a tension of 40 N and a frequency of 0.25 Hz. A 40 N load was chosen, as it was found in previous research to be a moderate load in the physiological range of the feline supraspinous ligament (Solomonow et al. 1998), and the results of this experiment will be used for a comparison with previous research involving 40-N static loading. A pretension of 1 N was applied before every single-cycle test or block of cyclic loading to establish the same baseline tension for all seven feline preparations. The loading sequence can be seen schematically in Figure 3.1.



$f = 0.25 \text{ Hz}$

Pre-Load Cycles: $P_1, P_2, P_3 = 40 \text{ N @ } f$

Rest Periods During Pre-Load: $r_{p1}, r_{p2}, r_{p3} = 10 \text{ min}$

Loading Periods: $L_1, L_2, \dots, L_N = 40 \text{ N @ } f \text{ for } 10 \text{ min}$

Rest Periods During Loading: $R_1, R_2, \dots, R_{N-1} = 10 \text{ min}$

Single-Cycle Tests During Recovery Period: $T_1, T_2, \dots, T_n = 40 \text{ N @ } f$

Rest Periods During Recovery: $r_0 = 10 \text{ min}, r_1 = 20 \text{ min}, r_2 = 30 \text{ min},$
 $r_i = 60 \text{ min for } i = 3 \text{ to } 8$

of Loading Periods: $N = 6$

(Note: Time Base not to Scale)

Figure 3.1: Loading sequence schematic and protocol parameters.

The protocol began with three single-cycle tests, each separated by ten minutes of rest. Averaging of the data from these three cycles yielded the pre-loading baseline for the Neuromuscular Neutral Zones (NNZs), EMG Peak Mean Absolute Value (EPMAV), and EMG Median Frequency (EMF). Following ten minutes of rest after the last test cycle,

the cyclic loading period began. Six blocks of ten-minute cyclic loading were applied, separated by ten minutes of rest in between each, resulting in a cumulative cyclic loading duration of 60 minutes. Following the last cyclic loading block, the seven-hour recovery period began, during which nine single-cycle tests were applied. The first, second, and third test cycles were applied ten, thirty, and sixty minutes into recovery, respectively. The remaining six cycles were then applied once every hour.

3.4 Data Processing

The raw EMG data was first divided by the amplifier gain (500) to yield the actual EMG values. 60 Hz noise was removed using a notch filter. A low pass filter was applied to raw displacement and tension data to filter unwanted noise. The raw displacement and tension data and any oscillations from the controller were found to be less than 5 Hz, which was the cutoff frequency set for the low pass filter.

In order to account for noise and signal artifacts that may have been present in the absence of loading, a baseline EMG Mean Absolute Value (EMAV) was found using pre-load EMG data. In the stretch phase of each test cycle, the onset of reflexive muscular activity was defined as the point in time at which the absolute value of EMG exceeded five times the baseline EMAV. The corresponding displacement and tension values at this point were defined as the onset displacement neuromuscular neutral zone (DNNZ) and tension neuromuscular neutral zone (TNNZ) thresholds, respectively. Similarly, in the release phase of each test cycle, the offset of reflexive muscular activity was defined as the point in time at which the absolute value of EMG dropped below five times the baseline. The corresponding displacement and tension values at this point were defined as the offset displacement and tension neutral zone thresholds, respectively. This procedure was implemented with a computer program and visually supervised to ensure that muscle spasms and other signal artifacts were not detected as neutral zone thresholds.

In order to obtain the EMG Peak Mean Absolute Value (EPMAV) in the period between the onset and offset neutral zone thresholds for each test cycle of the three lumbar levels, the EMG recorded from each lumbar level was full-wave rectified and smoothed with a 200 msec moving average filter. The moving average filter was moved up ten sample points following each averaging of the 200 msec window. This procedure

was repeated for the duration of the EMG cycle, and the EMAV of each 200 ms window was thus obtained for each cycle. The maximum EMAV value for each test cycle was defined as the EPMAV. The EPMAV values from the three pre-loading test cycles of each preparation were averaged together and used to normalize the subsequent EPMAV values in the cycles during the recovery period.

EMF was found for each single-cycle test in order to identify changes in motor unit recruitment (Solomonow et al. 1990). A 0.5-second window, centered at the peak load of each cycle, within which EMG was approximated as a stationary signal, was zero-padded on both sides. A Tukey window was applied to the zero-padded data, the power spectral density of the signal in this window was found via the fast Fourier transform, and the EMF was defined as the frequency that divides the area under the power spectral density in half.

Creep of the viscoelastic supraspinous ligament was calculated for periods during the loading, and for every single-cycle test during the 7-hour recovery period. In order to find these values, peak displacement of the L4-5 (location of hook application) supraspinous ligament of the first cycle and last cycle of each of the six loading blocks was found from the displacement data collected during the experiment. Peak displacement was also found for every single-cycle test during the recovery period. In order to obtain creep information, the peak displacement of the first cycle of the first loading block was defined as the baseline, and the percent change from baseline of the peak displacement data thereafter was found as

$$|(\text{loading or recovery cycle value} - \text{baseline value})/\text{baseline value}|*100$$

for the data of each feline preparation. The results of all feline subjects were then pooled to yield an average percent change from baseline. It is necessary to note that direct creep measurement or calculation was not possible in this experiment, as muscular contraction lessened the elongation of the ligament. Thus, the creep defined here is essentially true creep coupled with the EMG activity, which is the creep that exists in realistic situations.

3.5 Statistics

The DNNZ, TNNZ, EPMAV, and EMF data were inspected for normal probability distributions. If a distribution did not visually appear normal, an appropriate data transformation was applied to obtain such a distribution. A three-way repeated measures ANOVA was used to test for differences in the stretch and release phases of the DNNZ and TNNZ. The independent variables included time (pre-cyclic loading, recovery times), lumbar level of the multifidus (L3-4, L4-5, L5-6), and loading phase (stretch, release). All the dependent variables were tested for changes in time and lumbar level with a two-way repeated measures ANOVA. The independent variables were time (pre-static loading, recovery times) and lumbar level of the multifidus (L3-4, L4-5, L5-6), and the dependent variables included both stretch phase and release phase thresholds for the DNNZs and TNNZs. EPMAV and EMF were similarly tested for changes in time and lumbar level with a two-way repeated measures ANOVA, however in these tests stretch and release phases were not factors. All higher order factorial terms were included in the statistical models to test for interaction of the independent variables. Upon determining a significant interaction or main effect, pair-wise comparisons were performed using a post hoc Tukey Honest Significant Difference test. Level of significance was set as $p=0.05$.

3.6 Modeling

The mean \pm SD values of the DNNZ, TNNZ, and peak MAV during recovery for each lumbar level were fit with exponential-based models, as they represent the classical response of viscoelastic tissues (Solomonow et al. 2000).

The time-course of the DNNZ thresholds during the stretch phase and relaxation phase of the test cycles during the recovery period were described by:

$$DNNZ(t) = D_0 + (t - \tau_r)D_L \left(e^{-\frac{t-\tau_r}{\tau_1}} \right) + D_M \left(e^{-\frac{t-\tau_r}{\tau_2}} \right) \quad \{t \mid 120 \leq t \leq 530\}$$

Table 3.1 describes the coefficients and terms of this equation.

Coefficients/Terms of DNNZ(t)	Definition/Description
D_0	intercept of the displacement (mm)
D_L	affects rise amplitude of exponential dominating beginning of recovery period (mm/sec)
D_M	amplitude of decay dominating end of recovery period (mm)
τ_r	time of first recovery measurement (120 min)
τ_1	affects rates of rise and fall (sec)
τ_2	exponential time constant of decay dominating end of recovery period (min)
$(t - \tau_r) D_L \left(e^{-\frac{t - \tau_r}{\tau_1}} \right)$	allows for transient rise at beginning of recovery period
$D_M \left(e^{-\frac{t - \tau_r}{\tau_2}} \right)$	exponential decay dominating end of recovery period

Table 3.1: Definition/description of coefficients and terms of DNNZ(t).

The time-course of the TNNZ thresholds during the stretch phase and relaxation phase of the test cycles during the recovery period were described by:

$$TNNZ(t) = T_0 + (t - \tau_r) T_L \left(e^{-\frac{t - \tau_r}{\tau_3}} \right) + T_M \left(e^{-\frac{t - \tau_r}{\tau_4}} \right) \quad \{t | 120 \leq t \leq 530\}$$

Table 3.2 describes the coefficients and terms of this equation.

Coefficients/Terms of TNNZ(t)	Definition/Description
T_0	the intercept of the tension (N)
T_L	affects rise amplitude of exponential dominating beginning of recovery period (N/sec)
T_M	amplitude of decay dominating end of recovery period (N)
τ_r	time of first recovery measurement (120 min)
τ_3	affects rates of rise and fall (sec)
τ_4	exponential time constant of decay dominating end of recovery period (min)
$(t - \tau_r) T_L \left(e^{-\frac{t - \tau_r}{\tau_3}} \right)$	allows for transient rise at beginning of recovery period
$T_M \left(e^{-\frac{t - \tau_r}{\tau_4}} \right)$	exponential decay dominating end of recovery period

Table 3.2: Definition/description of coefficients and terms of TNNZ(t).

The time-course of the EPMAV during the recovery period was described by:

$$EPMAV(t) = \begin{cases} P_0 + P_L \left(e^{-\frac{t-\tau_r}{\tau_5}} \right) + P_M \left(1 - e^{-\frac{t-\tau_r}{\tau_6}} \right) & , t < \tau_d \\ P_0 + P_L \left(e^{-\frac{t-\tau_r}{\tau_5}} \right) + P_M \left(1 - e^{-\frac{t-\tau_r}{\tau_6}} \right) & \{t \mid 120 \leq t \leq 530\} \\ +(t - \tau_d) P_H \left(e^{-\frac{t-\tau_d}{\tau_7}} \right) & , t \geq \tau_d \end{cases}$$

Table 3.3 describes the coefficients and terms of this equation.

Coefficients/Terms of EPMAV(t)	Definition/Description
P_0	intercept of the peak MAV (mV)
P_L	amplitude of exponential decay dominating beginning of recovery period (mV)
P_M	amplitude of exponential increase following decay in beginning of recovery period (mV)
τ_r	time of first recovery measurement (120 min)
τ_d	time of onset of hyperexcitability (min)
τ_5	Exponential time constant of exponential decay dominating beginning of recovery period (min)
τ_6	Exponential time constant of exponential increase following decay in beginning of recovery period (min)
τ_7	Exponential time constant of hyperexcitability term dominating end of recovery period (min)
$P_L \left(e^{-\frac{t-\tau_r}{\tau_5}} \right)$	allows for exponential decay dominating beginning of recovery period
$P_M \left(1 - e^{-\frac{t-\tau_r}{\tau_6}} \right)$	allows for exponential increase following decay in beginning of recovery period
$(t - \tau_d) P_H \left(e^{-\frac{t-\tau_d}{\tau_7}} \right)$	hyperexcitability term with delayed onset dominating end of recovery period (equal to zero when $t < \tau_d$)

Table 3.3: Definition/description of coefficients and terms of EPMAV(t).

The time-course of the EMF smoothed with a 3-point moving average algorithm during the recovery period was described by:

$$EMF(t) = \begin{cases} F_0 + F_L \left(e^{-\frac{t-\tau_r}{\tau_8}} \right) + F_M \left(1 - e^{-\frac{t-\tau_r}{\tau_9}} \right) & , t < \tau_d \\ F_0 + F_L \left(e^{-\frac{t-\tau_r}{\tau_8}} \right) + F_M \left(1 - e^{-\frac{t-\tau_r}{\tau_9}} \right) & \{t | 120 \leq t \leq 530\} \\ +(t - \tau_d) F_H \left(e^{-\frac{t-\tau_d}{\tau_{10}}} \right) & , t \geq \tau_d \end{cases}$$

Table 3.4 describes the coefficients and terms of this equation.

Coefficients/Terms of EMF(t)	Definition/Description
F_0	intercept of the peak MF (Hz)
F_L	Amplitude of exponential decay dominating beginning of recovery period (Hz)
F_M	Amplitude of exponential increase following decay in beginning of recovery period (Hz)
τ_r	time of first recovery measurement (120 min)
τ_d	time of onset of hyperexcitability (min)
τ_8	exponential time constant of exponential decay dominating beginning of recovery period (min)
τ_9	exponential time constant of exponential increase following decay in beginning of recovery period (min)
τ_{10}	exponential time constant of hyperexcitability term dominating end of recovery period (min)
$F_L \left(e^{-\frac{t-\tau_r}{\tau_8}} \right)$	allows for exponential decay dominating beginning of recovery period
$F_M \left(1 - e^{-\frac{t-\tau_r}{\tau_9}} \right)$	allows for exponential increase following decay in beginning of recovery period
$(t - \tau_d) F_H \left(e^{-\frac{t-\tau_d}{\tau_{10}}} \right)$	hyperexcitability term with delayed onset dominating end of recovery period (equal to zero when $t < \tau_d$)

Table 3.4: Definition/description of coefficients and terms of EMF(t).

Levenberg-Marquardt nonlinear regression algorithms were used to generate the best fits, optimizing for the regression coefficient. In the case of EPMAV and EMF, which both had hyperexcitability terms, some manual interaction with the algorithms was necessary in choosing parameters to best approximate the model behavior.

CHAPTER 4
RESULTS

A typical recording of the raw EMG from L-3/4, L-4/5 and L-5/6, and the associated tension and displacement before, during, and after the cyclic loading period is shown in Figure 4.1.

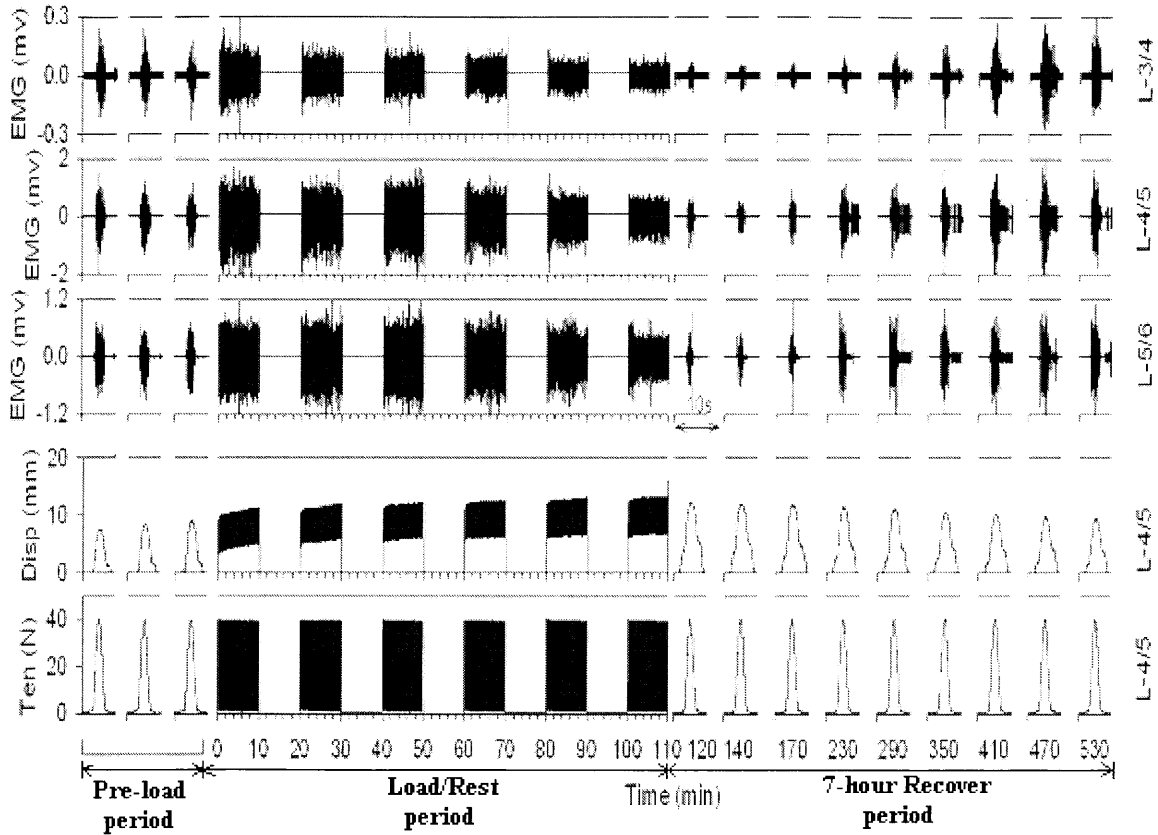


Figure 4.1: Typical recording of raw EMG from L3-4, L4-5, and L5-6, and corresponding tension and displacement vs. time during entire loading sequence.

A typical single cycle is shown in Figure 4.2 with the arrows indicating the initiation and cessation of EMG. The EMG MAV is also shown superimposed on each corresponding EMG signal.

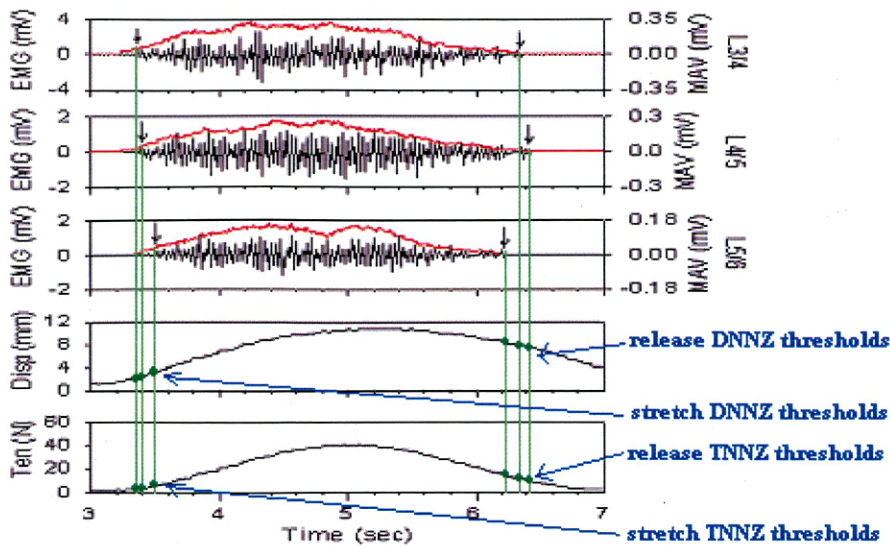


Figure 4.2: Typical recording of EMG from L3-4, L4-5, and L5-6 with superimposed MAV and arrows indicating initiation and cessation NNZ thresholds, and corresponding tension and displacement vs. time during single loading cycle.

4.1 Displacement Neuromuscular Neutral Zones (DNNZs)

The mean \pm the standard deviation for the pooled DNNZ thresholds for each of the lumbar levels in the stretch and release phases of the three pre-loading cycles and nine recovery cycles is shown in Figure 4.3. The DNNZs during stretch were significantly smaller ($P < 0.0001$) than their counterpart during relaxation.

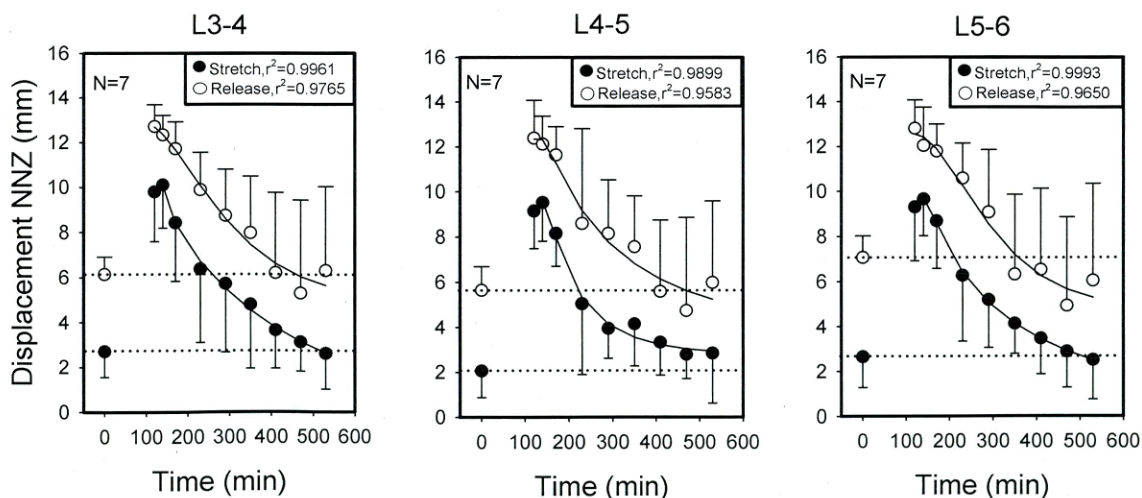


Figure 4.3: Mean \pm SD of DNNZ thresholds during stretch and release phases for data pooled across lumbar level vs. time with superimposed empirical models. Data points at time zero are baseline values from averaged pre-loading tests. Subsequent data is from recovery period.

Figure 4.4 shows the average percent difference (for all feline preparations and all lumbar levels) from the baseline values of the DNNZ thresholds over time. In order to calculate these values for each feline subject for each test cycle during the recovery period, the percent difference was calculated as

$$|(\text{recovery cycle value} - \text{original value})/\text{original value}|*100$$

for each lumbar level. These percent values were then averaged with values from corresponding cycles. The data from each feline subject was then pooled to yield the values represented in the figure.

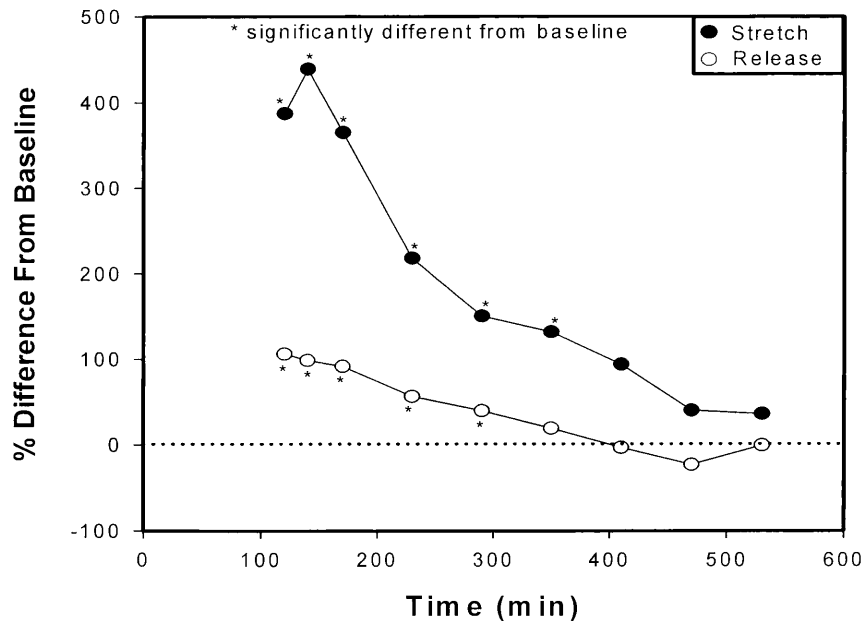


Figure 4.4: Average percent difference from baseline values vs. time of DNNZ thresholds. Negative percent values represent below-baseline data. Lumbar levels are combined. * next to data points indicates statistically significant difference from baseline, as revealed by the post hoc Tukey HSD test.

4.1.1 DNNZs in the Stretch Phase

The baseline mean \pm standard deviation DNNZ values from the three averaged pre-loading test cycles for the stretch phase of the L3-4, L4-5, and L5-6 lumbar levels were 2.70 ± 1.15 mm, 2.06 ± 1.17 mm, and 2.65 ± 1.37 mm, respectively. The mean

DNNZs showed significant change over time ($P < 0.0001$). During the stretch phase, in the 30 minutes immediately following loading, the DNNZs increased 3.6 to 4.6 fold above the baseline to 10.10 ± 1.92 mm, 9.52 ± 1.70 mm, and 9.65 ± 1.62 mm for the L3-4, L4-5, and L5-6 lumbar levels, respectively. This represented an average percent increase above the baseline values of 439 %. The DNNZs gradually returned to near normal by the end of the recovery period being 2.61 ± 1.60 mm, 2.85 ± 2.22 mm, and 2.50 ± 1.76 mm and were an average of 36 % above baseline values. A time and vertebral level interaction was not present ($P = 0.999$).

4.1.2 DNNZs in the Release Phase

The baseline mean \pm standard deviation DNNZ values from the three averaged pre-loading test cycles for the release phase of the L3-4, L4-5, and L5-6 lumbar levels were 6.13 ± 0.77 mm, 5.64 ± 1.06 mm, and 7.07 ± 0.96 mm, respectively. The mean DNNZ showed significant change over time ($P < 0.0001$). Immediately after loading, the DNNZs increased 1.8 to 2.2 fold above the baseline to 12.71 ± 0.98 mm, 12.38 ± 1.69 mm, and 12.79 ± 1.27 mm for the L3-4, L4-5, and L5-6 lumbar levels, respectively. This represented an average percent increase above baseline values of 106 %. The DNNZs gradually decreased to near baseline by the end of the recovery period being 6.30 ± 3.73 mm, 5.98 ± 3.61 mm, and 6.04 ± 4.31 mm, and were an average of 1 % below baseline values. Time and intervertebral level interaction was not present ($P = 0.998$).

4.2 Tension Neuromuscular Neutral Zones (TNNZs)

The mean \pm the standard deviation for the pooled TNNZ thresholds for each of the lumbar levels in the stretch and release phases of the three pre-loading cycles and nine recovery cycles is shown in Figure 4.5. It was determined that the TNNZ data did not fit a normal distribution, thus a square root data transformation was applied to obtain normality for the purpose of both the three-way and two-way repeated measures ANOVA tests. All figures represent the untransformed data. The TNNZ during stretch were significantly smaller ($P < 0.0001$) than their counterpart during relaxation.

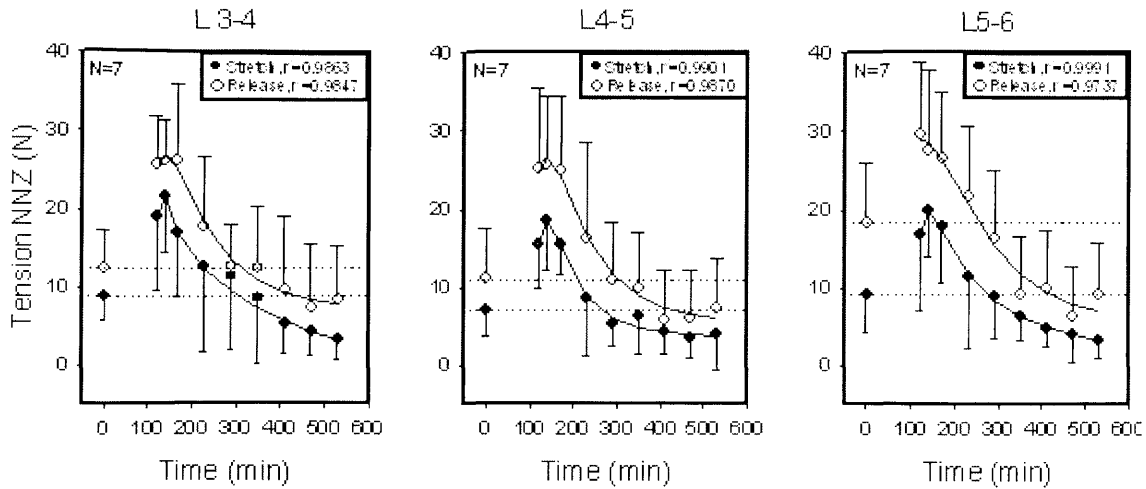


Figure 4.5: Mean \pm SD of TNNZ thresholds during stretch and release phases for data pooled across lumbar level vs. time with superimposed empirical models. Data points at time zero are baseline values from averaged pre – loading tests. Subsequent data is from recovery period.

Figure 4.6 shows the average percent difference (for all feline preparations and all lumbar levels) from baseline values of the TNNZ thresholds over time. These values were calculated as described in Section 4.1 for the DNNZ values.

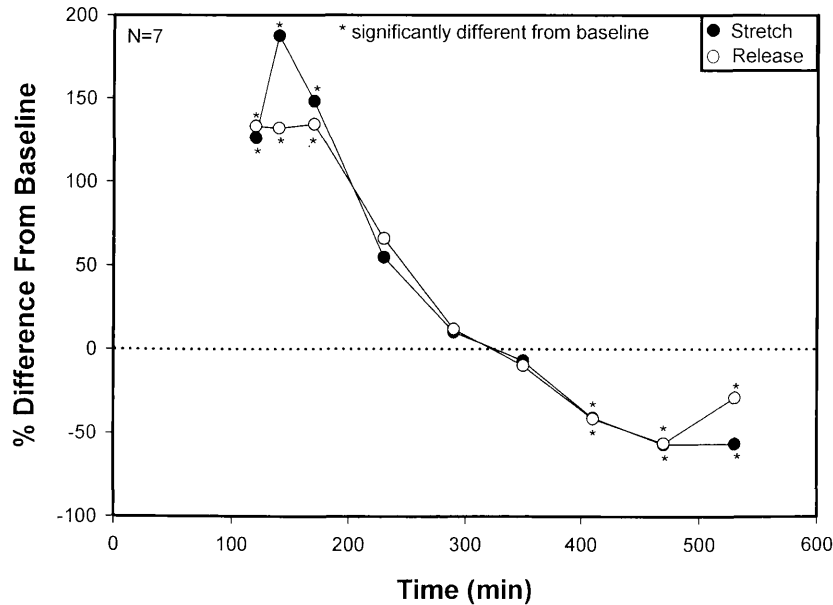


Figure 4.6: Average percent difference from baseline vs. time of TNNZ thresholds. Negative percent values represent below-baseline data. Lumbar levels are combined. * next to data points indicates statistically significant difference from baseline, as revealed by the post hoc Tukey HSD test.

4.2.1 TNNZs in the Stretch Phase

The baseline mean \pm standard deviation TNNZ values from the three averaged pre-loading test cycles for the stretch phase of the L3-4, L4-5, and L5-6 lumbar levels were 8.75 ± 3.06 N, 6.96 ± 3.31 N, and 9.14 ± 4.88 N, respectively. The mean TNNZ showed significant change over time ($P < 0.0001$) as well as significant difference between lumbar levels ($P = 0.0374$). During the stretch phase, in the 30 minutes immediately following loading, the TNNZs increased 2.2 to 2.7 fold above the baseline to 21.59 ± 7.21 N, 18.61 ± 6.29 N, and 19.78 ± 5.87 N for the L3-4, L4-5, and L5-6 lumbar levels, respectively. This represented an average increase of 126 % above baseline values. The TNNZs decreased to below the pre-loading baseline after the third hour of the recovery period for the L3-4 lumbar level, and after the second hour for the L4-5 and L5-6 lumbar levels. The TNNZs at the end of the recovery period were 1.8 to 2.8 fold below the baseline at 3.28 ± 2.65 N, 3.92 ± 4.65 N, and 3.23 ± 2.42 N for the L3-4, L4-5, and L5-6 lumbar levels, respectively. This represented an average decrease below the pre-loading baseline values of 57 % by the seventh hour of the recovery period. Time and intervertebral level interaction was not present ($P = 0.999$).

4.2.2 TNNZs in the Release Phase

The baseline mean \pm standard deviation TNNZ values from the three averaged pre-loading test cycles for the release phase of the L3-4, L4-5, and L5-6 lumbar levels were 12.36 ± 5.02 N, 11.12 ± 6.42 N, and 18.30 ± 7.77 N, respectively. The mean TNNZs showed significant change over time ($P < 0.0001$) as well as significant difference between lumbar levels ($P = 0.0354$). During the recovery period, the TNNZs increased 1.6 to 2.3 fold above the baseline to their maximum values within the first hour immediately after loading to 26.35 ± 9.55 N, 25.76 ± 8.74 , and 29.51 ± 9.25 for the L3-4, L4-5, and L5-6 lumbar levels respectively. Immediately after loading, there was an average increase of 133 % above the pre-loading baseline values. The TNNZs decreased to near pre-loading baseline by the third hour of the recovery period for the L3-4 and L4-5 lumbar levels, and to below the baseline after the second hour for the L5-6 lumbar level. The TNNZs at the end of the recovery period were 1.5 to 2 fold below the baseline at 8.38 ± 6.84 N, 7.28 ± 6.54 N, and 9.07 ± 6.74 N for the L3-4, L4-5, and L5-6 lumbar

levels, respectively. This represented an average decrease of 29 % below pre-loading baseline values. Time and intervertebral level interaction was not present ($P=0.984$).

4.3 Normalized EMG Peak Mean Absolute Value (EPMAV)

The mean \pm the standard deviation for the pooled normalized EPMAV data of each of the lumbar levels for the three pre-loading cycles and nine recovery cycles is shown in Figure 4.7. It was determined that the EPMAV data did not fit a normal distribution, thus a logarithmic (base 10) data transformation was applied to obtain normality for the purpose of both the three-way and two-way repeated measures ANOVA tests. All figures represent the untransformed data.

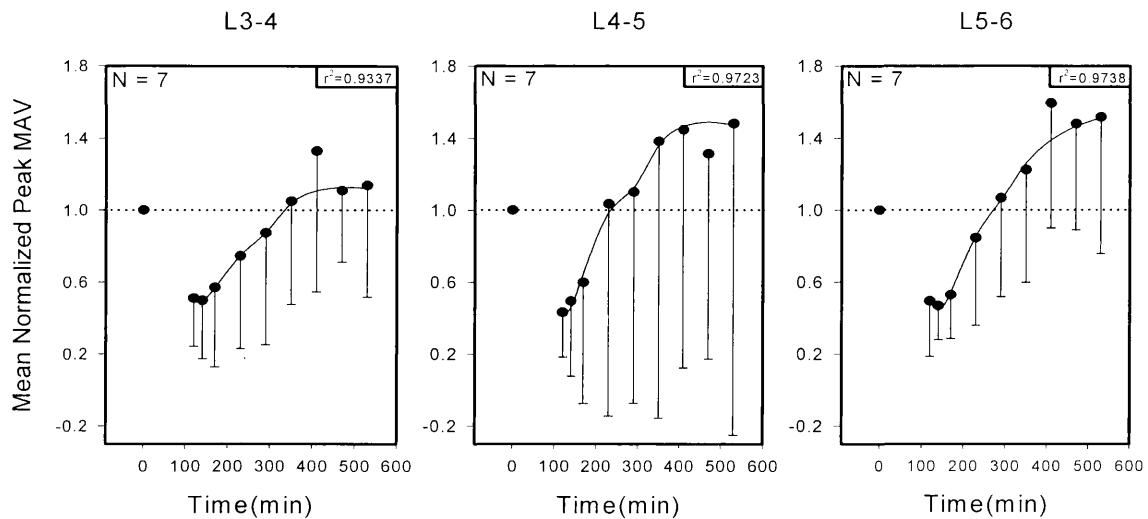


Figure 4.7: Mean \pm SD of EPMAV for data pooled across lumbar level vs. time with superimposed empirical models. Data points at time zero are baseline values from averaged pre – loading tests. Subsequent data is from recovery period.

Figure 4.8 shows the average percent difference (for all feline preparations and all lumbar levels) from the baseline of the EPMAV over time. These values were calculated as described in Section 4.1 for the DNNZ values; however the stretch and release phases were not factors in the calculations.

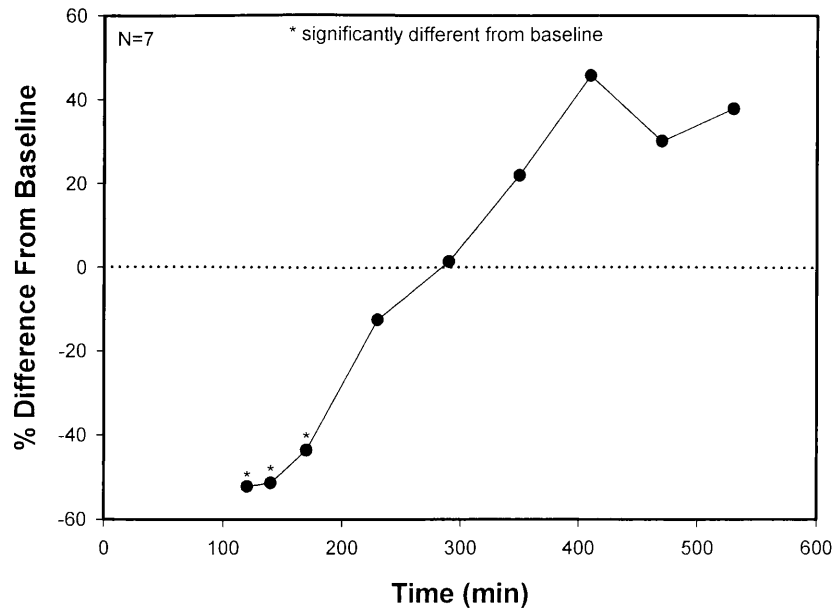


Figure 4.8: Average percent difference from baseline vs. time of EPMAV. Negative percent values represent below-baseline data. Lumbar levels are combined. * next to data points indicates statistically significant difference from baseline, as revealed by the post hoc Tukey HSD test.

The EPMAV from the three averaged pre-loading test cycles for the L3-4, L4-5, and L5-6 lumbar levels were used to normalize subsequent EPMAV of the same lumbar level in the recovery period. The EPMAV demonstrated a significant change over time ($P < 0.0001$). It decreased 2 to 2.3 fold below the baseline to its minimum value within 30 minutes into recovery for the three lumbar levels. Immediately after loading and thirty minutes into the recovery period, the EPMAV was an average of 52 % and 51 % below baseline values, respectively. The EPMAV fully recovered and exceeded its original baseline value after the third hour for L3-4, at about the second hour for L4-5, and after the second hour for L5-6, after which it increased until the end of the recovery period, where it was 1.1 to 1.5 fold above the baseline. The EPMAV for the three lumbar levels were an average of 38 % above the baseline values at the end of recovery. Time and intervertebral level interaction was not present ($P = 0.9998$).

4.4 EMG Median Frequency (EMF)

The mean \pm the standard deviation for the pooled EMF data of each of the lumbar levels for the three pre-loading cycles and nine recovery cycles is shown in Figure 4.9.

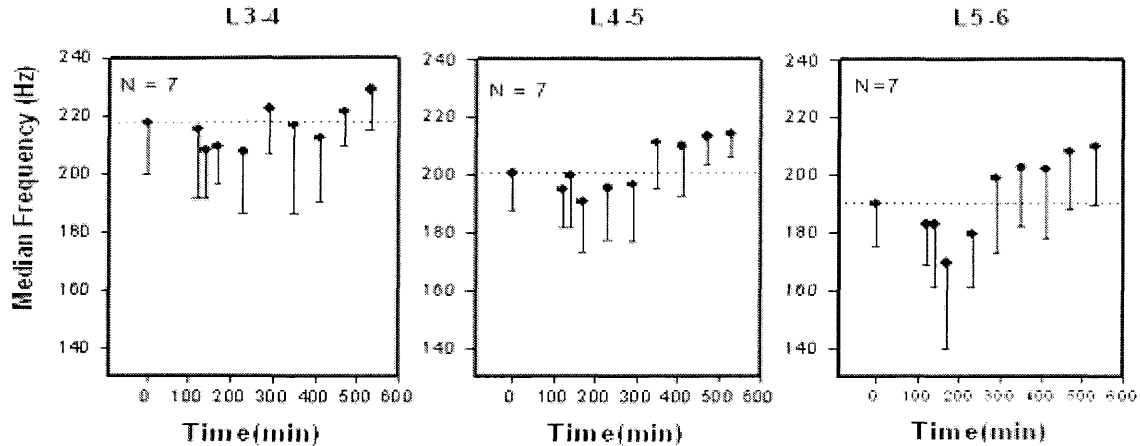


Figure 4.9: Mean \pm SD of EMF for data pooled across lumbar level vs. time. Data points at time zero are baseline value from averaged pre – loading tests. Subsequent data is from recovery period.

Figure 4.10 shows the mean \pm the standard deviation of the pooled median frequency smoothed with a 3-point moving average algorithm.

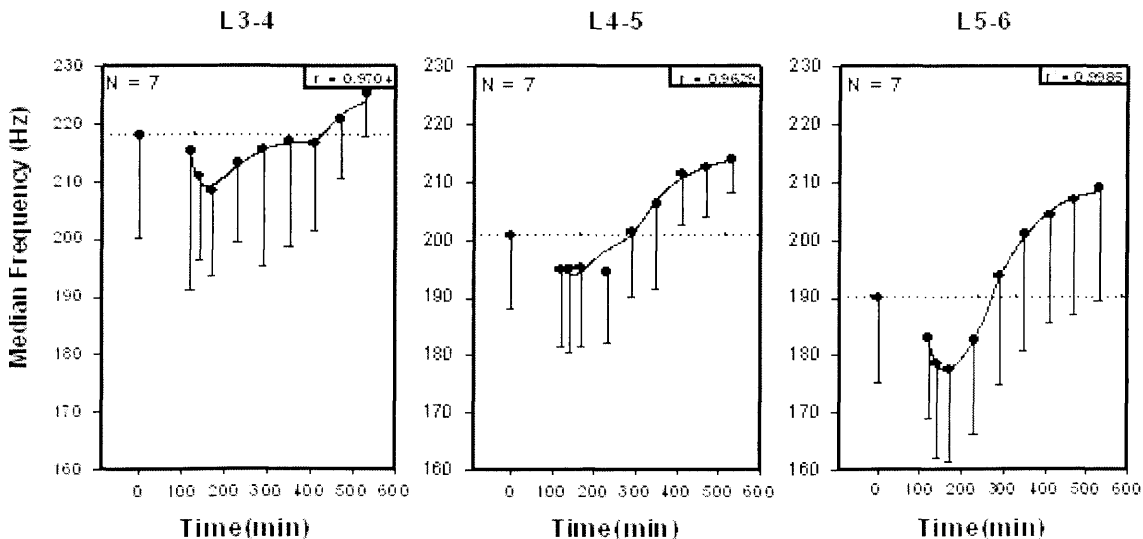


Figure 4.10: Mean \pm SD of EMF, smoothed with a 3-point moving average algorithm, for data pooled across lumbar level vs. time with superimposed empirical models. Data points at time zero are baseline values from averaged pre – loading tests. Subsequent data is from recovery period.

Figure 4.11 shows the average percent difference (for all feline preparations and all lumbar levels) from the baseline of the EMF over time. These values were calculated as described in section 4.1 for the DNNZ values; however the stretch and release phases were not factors in the calculations.

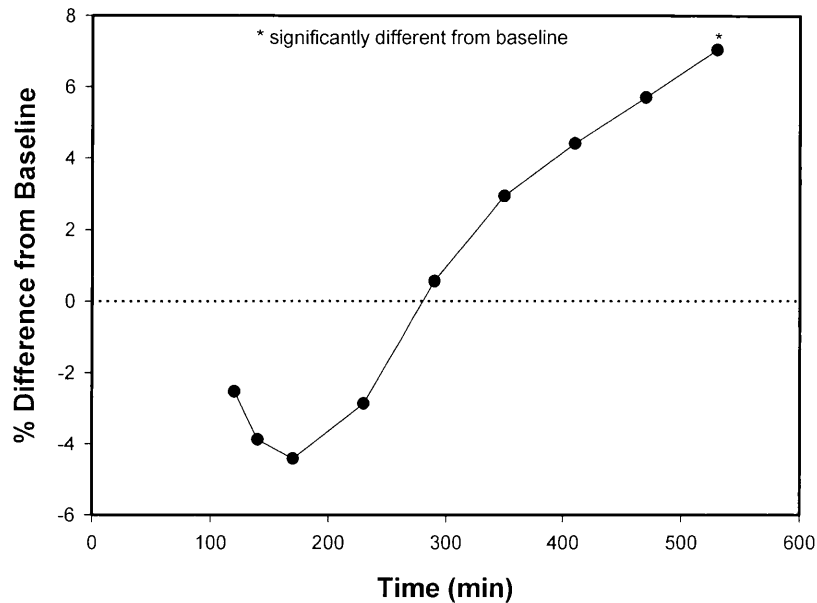


Figure 4.11: Average percent difference from baseline vs. time of EMF. Negative percent values represent below-baseline data. Lumbar levels are combined. * next to data points indicates statistically significant difference from baseline, as revealed by the post hoc Tukey HSD test.

The EMF demonstrated a significant change over time ($P < 0.0001$) as well as a significant difference between lumbar levels ($P < 0.0001$) that showed a decrease in EMF moving down in lumbar level from L3-4 to L5-6. The baseline mean \pm standard deviation EMF values from the three averaged pre-loading test cycles for the stretch phase of the L3-4, L4-5, and L5-6 lumbar levels were 218.10 ± 17.81 Hz, 200.71 ± 12.63 Hz, and 190.10 ± 14.89 Hz, respectively. Immediately after loading, the EMF values decreased an average of 2.5 % from baseline values to 215.40 ± 24.07 Hz, 194.75 ± 13.14 Hz, and 183.04 ± 14.16 Hz. The EMF for L3-4 and L5-6 continued to decrease exponentially until one hour into the recovery period to 208.43 ± 14.94 Hz and 177.46 ± 16.24 Hz, respectively. The L4-5 lumbar level EMF did not clearly show the

exponential decrease in the beginning of the recovery period, as it might have been masked by the large standard deviations. The average percent difference from baseline values at the first hour of recovery was 4.4 %. The EMF fully recovered by about the 4th hour for L3-4, the 3rd hour for L4-5 and after the 2nd hour for L5-6, after which it continued to exponentially increase above the baseline. At the 7th hour of recovery the MF was still significantly above the baseline being 225.45 ± 7.59 Hz, 213.87 ± 5.69 Hz, and 209.26 ± 19.64 Hz, for L3-4, L4-5, and L5-6, respectively. This represented an average percent increase from the baseline values of 7 %. Time and intervertebral level interaction was not present ($P=0.6343$).

4.5 Creep Response

Figure 4.12 shows the mean \pm standard deviation of the peak displacement vs. time from the beginning of loading until the end of recovery. The peak displacement was found for the first and last cycle of each of the six blocks of cyclic loading, as well as for each single-cycle test during the recovery period. On the time axis, “bob” denotes beginning of block and “eob” denotes end of block. Figure 4.13 shows the average percent difference of each peak displacement measurement for each feline preparation and all lumbar levels, from the first peak displacement measurement at time bob 1, with the same time axis format as in Figure 4.12. These values were calculated as described in section 3.4 of the experimental methods. In both figures, unpatterned shaded areas signify loading blocks, during which continuous cyclic loading is applied, and patterned shading areas signify the recovery period, during which nine single-cycle tests are applied throughout the 7-hour recovery period.

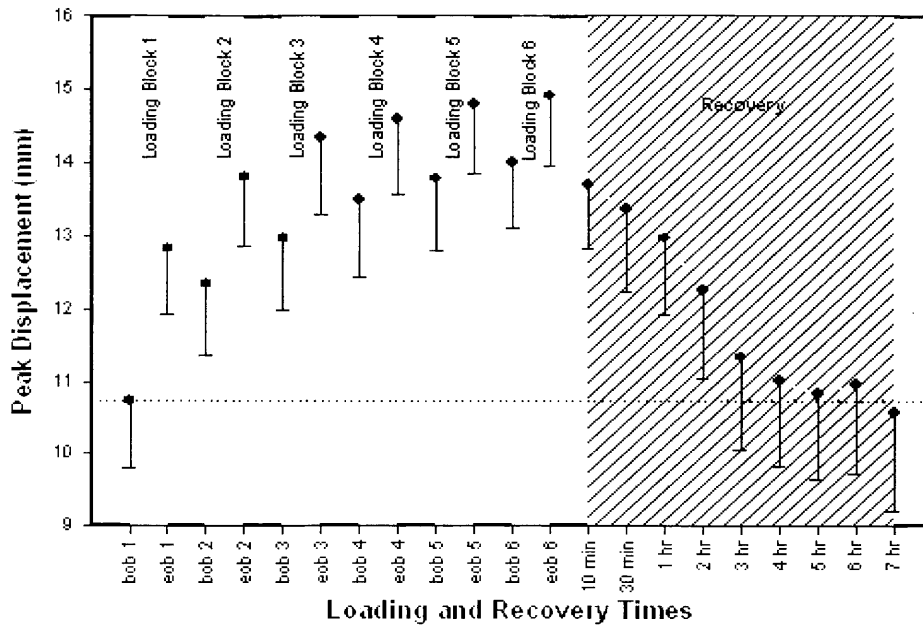


Figure 4.12: Mean \pm SD of peak displacement vs. time from beginning of loading until end of recovery. Only values from first and last cycle of each loading block are shown, as well as peak displacement for all single-cycle tests during recovery. On time axis, eob=end of block and bob=beginning of block.

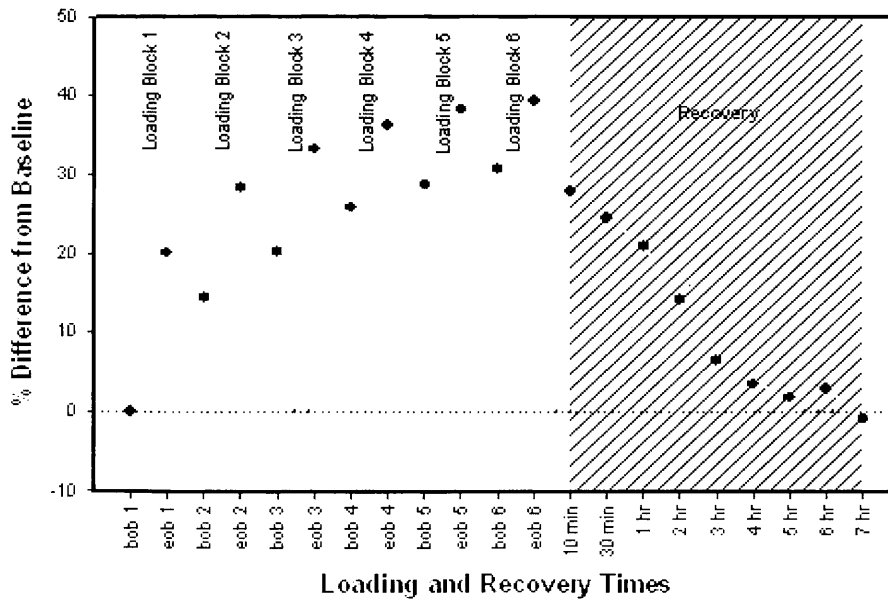


Figure 4.13: Average percent difference, of each peak displacement measurement for each feline preparation and all lumbar levels, from the first peak displacement measurement at time bob 1. Only values from first and last cycle of each loading block are shown, as well as for all single-cycle tests during recovery. On time axis, eob=end of block and bob=beginning of block.

It can be seen in both figures that creep increases from the beginning of each loading block to the end of each loading block. The ten minutes of rest in between each loading block allowed the creep to recover slightly before the beginning of the next loading block. A trend of increasing creep during the entire loading period can be seen. The creep reached an average of 40 % above the baseline values by the end of the loading period. Following the last loading block, the creep probably recovered exponentially, as it was seen to do so in a previous study of cyclic loading (Le et al. 2007), to the baseline by the end of recovery. At the end of recovery, the displacement was an average of 0.9 % below the baseline.

4.6 Modeling of DNNZ, TNNZ, EPMAV, and EMF Data

The empirical models derived for the DNNZ, TNNZ, EPMAV, and EMF are shown superimposed on their corresponding data in Figures 4.3, 4.5, 4.7, and 4.10, respectively.

4.6.1 DNNZ Model

Table 4.1 shows the DNNZ empirical model coefficient and time constant values for the stretch and release phase of each lumbar level, along with the corresponding regression coefficients, obtained via Levenberg-Marquart nonlinear regression algorithms.

DNNZ						
$DNNZ(t) = D_0 + (t - \tau_r)D_L \left(e^{-\frac{t-\tau_r}{\tau_1}} \right) + D_M \left(e^{-\frac{t-\tau_r}{\tau_2}} \right) \quad \{t 120 \leq t \leq 530\}$						
$\tau_r = 120$ (time at beginning of recovery)						
	Stretch			Release		
	L3-4	L4-5	L5-6	L3-4	L4-5	L5-6
D_0	0.5553	2.796	1.067	4.916	4.092	4.795
D_L	0.2818	0.1737	0.113	0.04202	0.07033	0.1531
D_M	9.165	6.314	8.223	7.768	8.247	7.75
τ_1	11.72	25.21	27.11	100	30.59	84.71
τ_2	276.2	108.5	234.1	143.4	208.7	50
r^2	0.9961	0.9899	0.9993	0.9765	0.9583	0.9650

Table 4.1: DNNZ empirical model coefficient and time constant values and regression coefficients for stretch and release phases of each lumbar level obtained by Levenberg-Marquart nonlinear regression algorithms.

4.6.2 TNNZ Model

Table 4.2 shows the TNNZ empirical model coefficient and time constant values for the stretch and release phase of each lumbar level, along with the corresponding regression coefficients, obtained via Levenberg-Marquart nonlinear regression algorithms.

TNNZ						
$TNNZ(t) = T_0 + (t - \tau_r)T_L \left(e^{-\frac{t-\tau_r}{\tau_3}} \right) + T_M \left(e^{-\frac{t-\tau_r}{\tau_4}} \right) \quad \{t 120 \leq t \leq 530\}$						
$\tau_r = 120$ (time at beginning of recovery)						
	Stretch			Release		
	L3-4	L4-5	L5-6	L3-4	L4-5	L5-6
T_0	-1.679	3.635	0.4939	6.833	5.056	5.695
T_L	0.7034	0.5453	0.4216	0.3301	0.3564	0.2063
T_M	20.74	11.9	16.36	18.54	19.93	23.11
τ_3	15.74	27.91	30.47	43.87	42.73	72.64
τ_4	280.4	100.9	224.4	143.1	130	130
r^2	0.9863	0.9901	0.9991	0.9847	0.9870	0.9737

Table 4.2: TNNZ empirical model coefficient and time constant values and regression coefficients for stretch and release phases of each lumbar level obtained by Levenberg-Marquart nonlinear regression algorithms.

4.6.3 EPMAV Model

Table 4.3 shows the EPMAV empirical model coefficient and time constant values for each lumbar level, along with the corresponding regression coefficients, obtained via Levenberg-Marquart nonlinear regression algorithms.

EPMAV			
$EPMAV(t) =$	$\left\{ \begin{array}{l} P_0 + P_L \left(e^{-\frac{t-\tau_r}{\tau_5}} \right) + P_M \left(1 - e^{-\frac{t-\tau_r}{\tau_6}} \right) \quad , t < \tau_d \\ P_0 + P_L \left(e^{-\frac{t-\tau_r}{\tau_5}} \right) + P_M \left(1 - e^{-\frac{t-\tau_r}{\tau_6}} \right) \quad \{t 120 \leq t \leq 530\} \\ + (t - \tau_d) P_H \left(e^{-\frac{t-\tau_d}{\tau_7}} \right) \quad , t \geq \tau_d \end{array} \right.$		
$\tau_r = 120$ (time at beginning of recovery)			
	L3-4	L4-5	L5-6
P_0	-2.748	-5.84	-2.78
P_L	3.257	6.282	3.283
P_M	3.74	7.029	4
P_H	0.002396	0.00477	0.002269
τ_5	52.56	36.72	44.31
τ_6	62.61	42.19	60
τ_7	169.9	171.9	400
τ_d	288.2	294.2	294.7
r^2	0.9337	0.9723	0.9738

Table 4.3: EPMAV empirical model coefficient and time constant values and regression coefficients for each lumbar level obtained by Levenberg-Marquart nonlinear regression algorithms.

4.6.4 EMF Model

Table 4.4 shows the EMF empirical model coefficient and time constant values for each lumbar level, along with the regression coefficients, obtained via Levenberg-Marquart nonlinear regression algorithms.

MF			
$EMF(t) =$	$\left\{ \begin{array}{ll} F_0 + F_L \left(e^{-\frac{t-\tau_r}{\tau_8}} \right) + F_M \left(1 - e^{-\frac{t-\tau_r}{\tau_9}} \right) & , t < \tau_d \\ F_0 + F_L \left(e^{-\frac{t-\tau_r}{\tau_8}} \right) + F_M \left(1 - e^{-\frac{t-\tau_r}{\tau_9}} \right) & \{t 120 \leq t \leq 530\} \\ + (t - \tau_d) F_H \left(e^{-\frac{t-\tau_d}{\tau_{10}}} \right) & , t \geq \tau_d \end{array} \right.$		
$\tau_r = 120$ (time at beginning of recovery)			
	L3-4	L4-5	L5-6
F_0	-205	-132.1	-50
F_L	419.2	328	232.5
F_M	422.7	335.5	250
F_H	0.11	0.09324	0.08514
τ_8	47.2	50.5	68
τ_9	49.4	53	80
τ_{10}	171.9	321.8	305.4
τ_d	420	290.5	230
r^2	0.9704	0.9629	0.9985

Table 4.4: EMF empirical model coefficient and time constant values and regression coefficients for each lumbar level obtained by Levenberg-Marquart nonlinear regression algorithms.

CHAPTER 5

DISCUSSION

The major findings of this investigation consist of the observations of profound changes in the Neuromuscular Neutral Zones and the motor control of muscular activity as a direct response to cyclic loading. Deficient passive and active spinal stability immediately after loading and a subsequent compensatory neural mechanism were found, as evidenced by the Displacement and Tension Neuromuscular Neutral Zones, EMG Peak Mean Absolute Value, EMG Median Frequency and creep of the lumbar viscoelastic tissues before and in the seven hours after loading. These findings are strongly supported by the statistical analysis. Empirical models of the above phenomena reveal classic physiological responses, as well as estimated recovery times from the chosen time constants, and new insight into the timing of the hyperexcitability response after cyclic loading.

Comparing the results of this study to a previous study (Youssef et al. 2008) in which static loading was used in the same protocol format revealed that cyclic loading is more deleterious to the neuromuscular system. Specifically, cyclic loading causes longer periods of instability and a more pronounced compensatory neural mechanism, as well as significant changes in motor unit recruitment which were found to be insignificant in static loading.

Finally, extrapolation of the data from the feline models used in this study to humans is analyzed theoretically.

5.1 Spinal Instability after Cyclic Loading

The ligamento-muscular stabilizing system of the spine is composed of passive stabilizers (ligaments, discs, facet capsules, etc.) and active stabilizers (muscles and reflex control/feedback) as discussed in Sections 2.1 and 2.2. The instability found as a result of cyclic loading discussed below is a result of deficiencies in both the passive and active stabilizing tissues.

Cyclic loading elicits a period of two to three hours post loading during which DNNZs and TNNZs are both elevated above pre-loading baseline values, exposing the

spine to instability. During the same two to three hours after loading, a significant decrease in the magnitude of muscular activity further compromises the stability of the spine. In addition, a concurrent decrease in the median frequency is witnessed, which suggests possible derecruitment of motor units. Thus, in addition to the deficient muscular activity, as seen by the decreased EMG amplitude, larger motor units may drop out of the active motor unit pool, resulting in less and smaller motor units in the active pool which are not capable of providing the pre-loading magnitude of muscle force to protect the spine.

The elevated DNNZs and TNNZs, deficient muscular activity, and possible derecruitment of active motor units all occur while there is still substantial creep in the lumbar viscoelastic tissues. From these findings, we can conclude that the spine is severely unstable with relatively no protection in preventing unwanted motion of spinal vertebrae relative to each other in the two to three hours after cyclic loading, exposing it to a high risk of injury.

The original activation of the multifidus muscles was shown to be a direct reflexive response to stretch of the ligaments and other viscoelastic tissues of the lumbar spine (Solomonow et al. 1998; Stubbs et al. 1998). In essence, elongation or loads above a certain threshold triggered reflexive muscular activity that stiffened the spine. It was further demonstrated that as tension-relaxation or creep develop in the spine over a period of flexion or loading, respectively, the trigger threshold for the reflex shifts substantially (Solomonow et al. 1999). The observed increase in the TNNZs and DNNZs after the cyclic loading period was probably the manifestation of the creep that developed in the viscoelastic tissue. Similarly, the reduction in the EPMAV was observed before and is a typical response to development of creep in the tissues during cyclic loading (Hoops et al. 2007; Le et al. 2007; Solomonow et al. 1998).

In addition to the evidence of deficient stability found in this study, it is also speculated that the flexion-extension motion caused loss of fluid in the discs of the spine and creep in the facet capsules and other viscoelastic tissues, although this was not measured. This further emphasizes the instability of the spine due to loss of resistance to motion of spinal vertebrae relative to each other.

5.2 Compensatory Neural Mechanism

Immediately after the two to three hour period of spinal instability described above, a compensatory neural mechanism emerged. The TNNZs decreased to below the pre-loading baseline, and the magnitude of muscle activity and the EMF increased exponentially and exceeded their respective pre-loading baselines. This compensation mechanism was still present at the end of the seven-hour recovery period.

The decrease in TNNZs represents the EMG triggering earlier and at a smaller-than-baseline tension during the stretch phase, and ceasing later and at a smaller-than-baseline tension during the release phase. Thus, EMG activity is triggered from smaller-than-normal perturbations about the neutral position, providing greater stability. Greater-than-baseline EPMAV signifies additional muscle force capable of stabilizing the spine. This is reinforced by the significantly greater-than-baseline EMF, which demonstrates recruitment of larger and more motor units, capable of providing greater-than-normal stabilizing forces, into the active motor unit pool.

The decreased TNNZs, elevated EPMAV, and additional recruitment of normally inactive motor units into the active motor unit pool all occur while there is still substantial creep in the lumbar viscoelastic tissues up to the seventh hour of recovery. Thus, this behavior could not be explained by a simple ligamento-muscular reflex. It is apparent that a different neural control mode is activated two to three hours after cyclic loading.

The different neural control modes could be associated with the clinical finding that tissue damage and the associated pain results in spasms, elevated muscular activity, and joint stiffness (Pedersen et al. 1956; van Dieen et al. 2003). The work of Woo et al. demonstrated that creep of the viscoelastic tissues is associated with microdamage in the collagen fibrils and the viscoelastic tissue could be considered damaged in this experiment. This neural control mode, therefore, is probably triggered by the tissue damage and the associated pain mechanism.

In summary, the major findings of decrease in TNNZs, and increase in EPMAV and EMF in late recovery is synergistic and all support the initiation of compensatory motor control by causing muscles to contract for smaller perturbations about the neutral

position, and increasing the muscle force while doing so, all during the manifestation of the harmful effects of the cyclic loading.

5.3 Statistical Analysis

Statistical analysis revealed strong support for the findings of this study. It was indeed shown that DNNZs, TNNZs, EPMAV, and EMF are functions of time over the recovery period as a result of cyclic loading. The rise in DNNZs and TNNZs immediately after loading was shown to be statistically significant. The post hoc analysis also revealed the slow recovery of DNNZs back to baseline at the end of recovery as significant. The compensation mechanism, in which the TNNZs dropped below baseline toward the end of recovery, was also statistically significant.

Post hoc analysis revealed that the reduction from baseline of the EPMAV immediately after loading was significant, however it failed to prove significant difference from baseline of the subsequent rise in late recovery. This may have been due to the large standard deviations produced by the variability of the hyperexcitability response between feline subjects. Further analysis of individual data revealed that some subjects had a more pronounced hyperexcitability response than others, and few had no hyperexcitability response at all. This could be due to many factors such as gender, genetics, age, hormones, and tolerance to loading, among many. Post hoc analysis of the EMF failed to show significant difference from baseline of the decrease immediately after loading, which could be due to the above stated factors. The analysis did, however, reveal that the increase above baseline toward the end of the recovery period was significant, confirming that more motor units were recruited, which would also give rise to the increase in EPMAV during this time.

Statistical analysis of the TNNZs revealed significance with lumbar level. The post hoc Tukey analysis revealed that the mean TNNZs were lower in L4-5 than in L3-4 and L5-6 multifidi. This is probably attributed to the position of the hook around the L4-5 supraspinal ligament, and suggests that more damage occurred to the L4-5 level of the ligament from direct application of the load

EMF also showed significance with lumbar level in the statistical analysis. In this case, the mean EMF decreased going down in lumbar level from L3-4 to L5-6. This can

probably be interpreted as the motor units being smaller and having slower conduction velocity at lower lumbar levels. EMF in a static loading study (Youssef et al. 2008) showed the same trend of EMF across lumbar levels, confirming that this trend is probably not an isolated finding.

5.4 Empirical Models

Exponential-based models were fit, using Marquart-Levenberg nonlinear regression algorithms, to the DNNZs, TNNZs, EPMAV, and EMF recovery data, as they represent the classical recovery response of viscoelastic tissues (Solomonow et al. 2000).

The DNNZ and TNNZ data fit the same general equation, having two exponential terms. This accounted for the small rise in neutral zones from the beginning of recovery to about thirty minutes into recovery, and the subsequent exponential decrease. It can be seen from the figures in Sections 4.1 and 4.2 that while DNNZ data, in general, returned to baseline by the seventh hour, TNNZ data was still below baseline by the seventh hour of recovery. It is speculated that TNNZs will eventually return to normal, and so a more appropriate choice of model for TNNZs would be to include a third exponential term that eventually increases back to the baseline and stays there. However, the data at the end of the seven hours of recovery did not clearly show any sign of trending toward baseline. Due to the limited recovery time, there was an insufficient amount of data points to accurately fit such a component to the model, thus the model shown is intended only to depict the data during the specified experiment time, and not afterward. Thus, the approximate time of complete recovery of the TNNZs cannot be predicted from the current model.

The EPMAV and EMF data fit the same general equation, having three exponential terms, one of which is delayed in time. The same general equation was used for these two phenomena based on their dependent relationship. In the absence of muscle fatigue, as we have in this study, a decrease in EMF, and thus derecruitment of motor units, yielded a decrease in EPMAV, and an increase in EMF, and thus recruitment of more motor units, yielded an increase in EPMAV. The multiple exponential terms in the recovery period have physiological significance. It has been suggested that a biexponential recovery model is more suitable than a single-exponential model to

describe recovery behavior of viscoelastic tissues composed of those with more viscous properties (discs) and those with more elastic properties (ligaments) (Gedalia et al. 1999). When loaded, discs and ligaments both lose fluids. However, reuptake of these fluids occurs rapidly in ligaments, but slowly in discs (Adams et al. 1987). This gives rise to the later exponential hyperexcitability component in recovery of reflexive muscular activity. The initiation time of this hyperexcitability component for the empirical models was visually approximated from the data in both the EPMAV, ranging from 288.2 to 294.7 minutes into recovery, and EMF, ranging from 230 to 420 minutes into recovery, and may not be exact. This term eventually decays to a steady-state value, and thus approximate times at which EPMAV and EMF recover fully can be predicted. The EPMAV full recovery time for the three lumbar levels was within approximately 24 to 48 hours, which concurs with a previous study (Solomonow et al. 2003b) in which muscular activity was predicted to recover to the original baseline within 48 hours. The EMF full recovery time for the three lumbar levels was also within 24 to 48 hours. It should be noted here also that the empirical models for the EPMAV and EMF were meant to closely approximate the behavior of the phenomena during the specified recovery time (seven hours), and not to accurately estimate the behavior thereafter. All hyperexcitability terms were found to decay to some steady-state values in a reasonable amount of time, however these steady-state values were either slightly above or slightly below the pre-loading baseline. Changing several of the coefficients would have allowed the steady-state values to be equal to pre-loading baseline values, however doing this would have no bearing on the time it takes to reach these values and would also lead to poor fits for the first seven hours of recovery, whose modeling was the main objective. Thus, the approximate time it took to reach respective steady-state values was defined as the full recovery time.

5.5 Comparison of Cyclic and Static Loading

A previous study (Youssef et al. 2008) used the same loading sequence protocol as in this study, but replaced the six ten-minute blocks of 40-N sinusoidal loading with six ten-minute blocks of 40-N static loading. In comparing the results of this study with those of the static loading study, it was found that cyclic loading is more hazardous, with

respect to spinal stability and damage inflicted. In the stretch phase of the single-cycle tests during recovery, the DNNZs were found to increase a greater percentage amount above baseline immediately after loading in the cyclic loading experiment. In both the stretch and release phases, the TNNZs were found to increase a substantially greater percentage amount above baseline immediately after loading in the cyclic experiment, and took longer to decrease below the baseline than in the static experiment. Thus, immediately after loading, the spine is at a greater risk from injury after cyclic loading due to shorter durations of EMG protective reflexes during flexion-extension work or exercises. In addition, the neural compensation mechanism initiated later during recovery in cyclic loading, as seen by the comparison of TNNZ results, leaving the spine unprotected for a longer period of time than in the static loading experiment.

EPMAV decreased to below the baseline immediately after loading in the cyclic experiment, whereas the EPMAV did not reach its minimum value below baseline until about one hour into the recovery period in the static experiment. This indicates that the spine is more unstable in the first hour of recovery for the cyclic experiment than in the static experiment due to more deficient protective muscular force during this time.

A very interesting result was found in comparing the median frequency results of both experiments. While the EMF results in cyclic loading showed statistical significance over time in the recovery period, the results in the static experiment failed to do so. The EMF also never exceeded the baseline for the static experiment, whereas significant increase above the baseline was shown in the end of the recovery period for the cyclic loading. This indicates that motor units were not derecruited as an immediate result of static loading. Also, a compensatory mechanism, in which more motor units than normal are recruited, was not employed in the static loading case. This suggests that the neural compensatory mechanism in the static case, rather than recruiting more motor units for additional force, caused the existing active motor units to fire at a higher rate, thus increasing the amplitude of the spatio-temporal summation of action potentials, and hence EPMAV. In the case of cyclic loading, motor units had to be recruited for additional muscle force, indicating that the existing active motor units were not sufficient to provide the needed compensatory muscle force.

In summary, cyclic loading leaves the spine more unstable immediately after loading, and unstable for a longer period of time than in static loading. It is also evident that more damage was caused in the cyclic loading case, as motor units may have been derecruited immediately after loading, and the need for more active motor units arises several hours into the recovery period in order to compensate for the laxity in the viscoelastic tissues of the spine.

These results concur with findings from several previous studies. A previous study (Courville et al. 2005) showed that static loading at a 1:1 work to rest ratio (10 minutes work: 10 minutes rest) for 60 minutes at a moderate load (40 N), as used in this study, did not create a neuromuscular disorder, as the EMG amplitude did not exceed its baseline over the 7-hour recovery period. Conversely, a previous study of cyclic loading (Hoops et al. 2007), in which an identical loading protocol as this study was used, showed the development of an acute neuromuscular disorder with a delayed hyperexcitability component in the later part of the 7-hour recovery period.

5.6 Extrapolation/Applicability of Data from Feline Model to Human

It is necessary to take into consideration that feline, and not human, models were used in this study. Several differences exist between the feline (quadruped) and human (biped) species including size and orientation of the gravity vector with respect to the spine (axial for humans while sitting and standing, 90 degrees for felines). In addition, hormonal and metabolic differences between the two species and prior work history in humans may have bearing on the conclusions made. With respect to the size difference, the response time in humans may be greater because action potentials have longer distances to travel to and from the spinal cord (Stubbs et al. 1998). In addition, the feline spinal discs are much smaller than those of humans, which may lead to faster fluid loss in felines, and thus the time delay of the hyperexcitability component may be smaller or nonexistent in humans (Solomonow et al. 1999).

Although extrapolation of the results to humans is not simple and straightforward, recent studies have slowly been confirming the results from this and other *in vivo* feline studies in humans. A previous study (Solomonow et al. 1998) confirmed that a ligamento-muscular reflex exists from the supraspinous ligament to the multifidi in

humans. It has also been shown that static and cyclic loading of spinal and knee ligaments in humans elicit spasms during loading and a neuromuscular disorder after loading (Chu et al. 2003; Li et al. 2007; Olson et al. 2004; Sbriccoli et al. 2005; Solomonow et al. 2003a). The microdamage in the viscoelastic tissues inflicted in this study could be classified as sub-clinical for such physiological loads and displacements, yet was shown in humans to result in stiffening of the spine several hours after the work was completed (Granata and Marras 2000). Similarly, previous studies (Dickey et al. 2003; Li et al. 2007; Olson et al. 2006; Olson et al. 2004) found that such significant changes in muscular activity occur after moderate and mild cyclic loading in humans. In essence, the above cited research also validates that the observations made in this study, using an *in vivo* feline model, are also seen in humans subjected to similar loading conditions, and that mild loading dose-duration can trigger such muscular responses.

It is suggested that physiological mechanisms such as the ligamento-muscular reflex, creep of viscoelastic tissues, and mechanoreceptor excitability will exhibit the same general pattern in both species, however, the timing and extent of certain phenomena as a result of cyclic loading, including loss of reflexive muscular activity, may be different (Solomonow et al. 1999).

CHAPTER 6

CONCLUSION

In summary, the data obtained in this experiment and the conclusions that can be drawn from it are as follows:

1. A sequence of cyclic loading at a 1:1 work to rest ratio, for a moderate cumulative loading duration and at a moderate load significantly increases the tension and displacement neuromuscular neutral zones while decreasing peak muscular activity and possibly derecruiting normally-active motor units in the two to three hours immediately after the loading.
2. The lumbar spine is exposed to significant reduction of stability control and high risk of injury in that period due to laxity in the lumbar viscoelastic tissues and deficient muscular activation and force.
3. A compensatory neural control mechanism, different from a simple ligamento-muscular reflex, triggers by the third hour after loading and significantly enhances the magnitude and timing of the muscular contributions, and recruits additional force-providing motor units into the active motor pool, while allowing the viscoelastic tissues to recover from the induced creep for the following hours.
4. Hyperexcitability seen in the enhanced magnitude of muscular activity and the activity of additional active motor units is predicted to fully recover to normal levels within 24 to 48 hours of cessation of loading.
5. Cyclic loading leaves the spine more unstable and for a longer period of time immediately after loading than does static loading, as seen by the greater increase in neutral zones and the later initiation of a neural compensatory mechanism. Cyclic loading is also more damaging than static loading for the above reasons and in that motor units are possibly derecruited following loading, and the compensatory mechanism requires additional motor units to be recruited, whereas this was not observed in static loading.

This study is relevant in the understanding of the motor control mechanisms of the lumbar spine during and after exposure to moderate cyclic loading. It is a step in the direction of designing optimal work/rest schedules and conditions for workers that would prevent injury due to the instability in the spine described above. Future work needs to be done to design these optimal conditions.

REFERENCES CITED

- Adams, M. (2007). Re: Spine stability: the six blind men and the elephant. *Clin Biomech (Bristol, Avon)* 22:486; author reply 487-488.
- Adams, M. A., Dolan, P. and Hutton, W. C. (1987). Diurnal variations in the stresses on the lumbar spine. *Spine* 12:130-137.
- Andersson, G. B. (1981). Epidemiologic aspects on low-back pain in industry. *Spine* 6:53-60.
- Baratta, R., Solomonow, M., Zhou, B. H., Letson, D., Chuinard, R. and D'Ambrosia, R. (1988). Muscular coactivation. The role of the antagonist musculature in maintaining knee stability. *Am J Sports Med* 16:113-122.
- Bellemere, F., and Grassino, A. (1979). The fatigue and recovery of the human diaphragm, in *Proc. Int. Congr. Electrophysiol. Kinesiol.*, 4th, 74-75.
- Chu, D., LeBlanc, R., D'Ambrosia, P., D'Ambrosia, R., Baratta, R. V. and Solomonow, M. (2003). Neuromuscular disorder in response to anterior cruciate ligament creep. *Clin Biomech (Bristol, Avon)* 18:222-230.
- Courville, A., Sbriccoli, P., Zhou, B. H., Solomonow, M., Lu, Y. and Burger, E. L. (2005). Short rest periods after static lumbar flexion are a risk factor for cumulative low back disorder. *J Electromyogr Kinesiol* 15:37-52.
- Crisco, J. J., Chelikani, S., Brown, R. K. and Wolfe, S. W. (1997). The effects of exercise on ligamentous stiffness in the wrist. *J Hand Surg [Am]* 22:44-48.
- Dickey, J. P., McNorton, S. and Potvin, J. R. (2003). Repeated spinal flexion modulates the flexion-relaxation phenomenon. *Clin Biomech (Bristol, Avon)* 18:783-789.
- Ekstrom, L., Kaigle, A., Hult, E., Holm, S., Rostedt, M. and Hansson, T. (1996). Intervertebral disc response to cyclic loading--an animal model. *Proc Inst Mech Eng [H]* 210:249-258.
- Eversull, E., Solomonow, M., Bing He Zhou, E. E., Baratta, R. V. and Zhu, M. P. (2001). Neuromuscular neutral zones sensitivity to lumbar displacement rate. *Clin Biomech (Bristol, Avon)* 16:102-113.
- Gedalia, U., Solomonow, M., Zhou, B. H., Baratta, R. V., Lu, Y. and Harris, M. (1999). Biomechanics of increased exposure to lumbar injury caused by cyclic loading. Part 2. Recovery of reflexive muscular stability with rest. *Spine* 24:2461-2467.

- Givens, M. W. and Teeple, J. B. (1978). Myoelectric frequency changes in children during static force production. *Electroencephalogr Clin Neurophysiol* 45:173-177.
- Granata, K. P. and Marras, W. S. (2000). Cost-benefit of muscle cocontraction in protecting against spinal instability. *Spine* 25:1398-1404.
- Granata, K. P., Rogers, E. and Moorhouse, K. (2005). Effects of static flexion-relaxation on paraspinal reflex behavior. *Clin Biomech (Bristol, Avon)* 20:16-24.
- Hirokawa, S., Solomonow, M., Lu, Y., Lou, Z. P. and D'Ambrosia, R. (1992). Anterior-posterior and rotational displacement of the tibia elicited by quadriceps contraction. *Am J Sports Med* 20:299-306.
- Hirokawa, S., Solomonow, M., Luo, Z., Lu, Y., Baratta, R.V. (1991). Muscular co-contraction. *J of Electromyogr and Kinesiol* 1:199-208.
- Hoogendoorn, W. E., Bongers, P. M., de Vet, H. C., Douwes, M., Koes, B. W., Miedema, M. C., Ariens, G. A. and Bouter, L. M. (2000). Flexion and rotation of the trunk and lifting at work are risk factors for low back pain: results of a prospective cohort study. *Spine* 25:3087-3092.
- Hoops, H., Zhou, B. H., Lu, Y., Solomonow, M. and Patel, V. (2007). Short rest between cyclic flexion periods is a risk factor for a lumbar disorder. *Clin Biomech (Bristol, Avon)* 22:745-757.
- Kadefors, R., Kaiser, E. and Petersen, I. (1968). Dynamic spectrum analysis of myopotentials and with special reference to muscle fatigue. *Electromyography* 8:39-74.
- Karajcarski, S., Wells, R. (2006). The time variation pattern of mechanical exposure and the reporting of low back pain. *Theoretical Issues in Ergonomic Science* 1-27.
- LaBry, R., Sbriccoli, P., Zhou, B. H. and Solomonow, M. (2004). Longer static flexion duration elicits a neuromuscular disorder in the lumbar spine. *J Appl Physiol* 96:2005-2015.
- Le, P., Solomonow, M., Zhou, B. H., Lu, Y. and Patel, V. (2007). Cyclic load magnitude is a risk factor for a cumulative lower back disorder. *J Occup Environ Med* 49:375-387.
- Li, L., Patel, N., Solomonow, D., Le, P., Hoops, H., Gerhardt, D., Johnson, K., Zhou, B. H., Lu, Y. and Solomonow, M. (2007). Neuromuscular response to cyclic lumbar twisting. *Hum Factors* 49:820-829.
- Lindstrom, L., Magnusson, R. and Petersen, I. (1970). Muscular fatigue and action potential conduction velocity changes studied with frequency analysis of EMG signals. *Electromyography* 10:341-356.

- Lu, D., Solomonow, M., Zhou, B., Baratta, R. V. and Li, L. (2004). Frequency-dependent changes in neuromuscular responses to cyclic lumbar flexion. *J Biomech* 37:845-855.
- Lucas, D. B., Bresler, B. and Florence Hellman Ehrman Endowment Fund for Orthopedic Research. (1961). *Stability of the ligamentous spine*. Biomechanics Laboratory, University of California, San Francisco.
- Magora, A., Gonen, B., Eimerl, M. S. and Magora, F. (1976). Electrophysiological manifestations of isometric contraction sustained to maximal fatigue in healthy humans. *Electromyogr Clin Neurophysiol* 16:309-334.
- Manchikanti, L. (2000). Epidemiology of low back pain. *Pain Physician* 3:167-192.
- Marras, W. S. (2000). Occupational low back disorder causation and control. *Ergonomics* 43:880-902.
- Marras, W. S., Lavender, S. A., Leurgans, S. E., Fathallah, F. A., Ferguson, S. A., Allread, W. G. and Rajulu, S. L. (1995). Biomechanical risk factors for occupationally related low back disorders. *Ergonomics* 38:377-410.
- Marras, W. S., Lavender, S. A., Leurgans, S. E., Rajulu, S. L., Allread, W. G., Fathallah, F. A. and Ferguson, S. A. (1993). The role of dynamic three-dimensional trunk motion in occupationally-related low back disorders. The effects of workplace factors, trunk position, and trunk motion characteristics on risk of injury. *Spine* 18:617-628.
- McGill, S. M. (1997). The biomechanics of low back injury: implications on current practice in industry and the clinic. *J Biomech* 30:465-475.
- Navar, D., Zhou, B. H., Lu, Y. and Solomonow, M. (2006). High-repetition cyclic loading is a risk factor for a lumbar disorder. *Muscle Nerve* 34:614-622.
- Olson, M., Solomonow, M. and Li, L. (2006). Flexion-relaxation response to gravity. *J Biomech* 39:2545-2554.
- Olson, M. W., Li, L. and Solomonow, M. (2004). Flexion-relaxation response to cyclic lumbar flexion. *Clin Biomech (Bristol, Avon)* 19:769-776.
- Olson, M. W., Li, L. and Solomonow, M. (2007). Interaction of viscoelastic tissue compliance with lumbar muscles during passive cyclic flexion-extension. *J Electromyogr Kinesiol.*
- Omino, K. and Hayashi, Y. (1992). Preparation of dynamic posture and occurrence of low back pain. *Ergonomics* 35:693-707.
- Panjabi, M. M. (1992). The stabilizing system of the spine. Part II. Neutral zone and instability hypothesis. *J Spinal Disord* 5:390-396; discussion 397.

- Panjabi, M. M. (1996). Low Back Pain and Spinal Stability, in *Low Back Pain: A Scientific and Clinical Overview*, American Academy of Orthopedic Surgeons, Rosemont, Il, 367-384.
- Pedersen, H. E., Blunck, C. F. and Gardner, E. (1956). The anatomy of lumbosacral posterior rami and meningeal branches of spinal nerve (sinu-vertebral nerves); with an experimental study of their functions. *J Bone Joint Surg Am* 38-A:377-391.
- Preuss, R. and Fung, J. (2005). Can acute low back pain result from segmental spinal buckling during sub-maximal activities? A review of the current literature. *Man Ther* 10:14-20.
- Punnett, L., Fine, L. J., Keyserling, W. M., Herrin, G. D. and Chaffin, D. B. (1991). Back disorders and nonneutral trunk postures of automobile assembly workers. *Scand J Work Environ Health* 17:337-346.
- Punnett, L. and Wegman, D. H. (2004). Work-related musculoskeletal disorders: the epidemiologic evidence and the debate. *J Electromyogr Kinesiol* 14:13-23.
- Reeves, N. P., Narendra, K. S. and Cholewicki, J. (2007). Spine stability: the six blind men and the elephant. *Clin Biomech (Bristol, Avon)* 22:266-274.
- Sbriccoli, P., Solomonow, M., Zhou, B. H., Baratta, R. V., Lu, Y., Zhu, M. P. and Burger, E. L. (2004a). Static load magnitude is a risk factor in the development of cumulative low back disorder. *Muscle Nerve* 29:300-308.
- Sbriccoli, P., Solomonow, M., Zhou, B. H., Lu, Y. and Sellards, R. (2005). Neuromuscular response to cyclic loading of the anterior cruciate ligament. *Am J Sports Med* 33:543-551.
- Sbriccoli, P., Yousuf, K., Kupershtein, I., Solomonow, M., Zhou, B. H., Zhu, M. P. and Lu, Y. (2004b). Static load repetition is a risk factor in the development of lumbar cumulative musculoskeletal disorder. *Spine* 29:2643-2653.
- Shin, G. and Mirka, G. A. (2007). An in vivo assessment of the low back response to prolonged flexion: Interplay between active and passive tissues. *Clin Biomech (Bristol, Avon)* 22:965-971.
- Silverstein, B. and Clark, R. (2004). Interventions to reduce work-related musculoskeletal disorders. *J Electromyogr Kinesiol* 14:135-152.
- Silverstein, B. A., Fine, L. J. and Armstrong, T. J. (1986). Hand wrist cumulative trauma disorders in industry. *Br J Ind Med* 43:779-784.

- Solomonow, M., Baratta, R. V., Banks, A., Freudenberger, C. and Zhou, B. H. (2003a). Flexion-relaxation response to static lumbar flexion in males and females. *Clin Biomech (Bristol, Avon)* 18:273-279.
- Solomonow, M., Baratta, R. V., Zhou, B. H., Burger, E., Zieske, A. and Gedalia, A. (2003b). Muscular dysfunction elicited by creep of lumbar viscoelastic tissue. *J Electromyogr Kinesiol* 13:381-396.
- Solomonow, M., Baten, C., Smit, J., Baratta, R., Hermens, H., D'Ambrosia, R. and Shoji, H. (1990). Electromyogram power spectra frequencies associated with motor unit recruitment strategies. *J Appl Physiol* 68:1177-1185.
- Solomonow, M., Eversull, E., He Zhou, B., Baratta, R. V. and Zhu, M. P. (2001). Neuromuscular neutral zones associated with viscoelastic hysteresis during cyclic lumbar flexion. *Spine* 26:E314-324.
- Solomonow, M., He Zhou, B., Baratta, R. V., Lu, Y., Zhu, M. and Harris, M. (2000). Biexponential recovery model of lumbar viscoelastic laxity and reflexive muscular activity after prolonged cyclic loading. *Clin Biomech (Bristol, Avon)* 15:167-175.
- Solomonow, M., Zhou, B. H., Baratta, R. V., Lu, Y. and Harris, M. (1999). Biomechanics of increased exposure to lumbar injury caused by cyclic loading: Part 1. Loss of reflexive muscular stabilization. *Spine* 24:2426-2434.
- Solomonow, M., Zhou, B. H., Harris, M., Lu, Y. and Baratta, R. V. (1998). The ligamento-muscular stabilizing system of the spine. *Spine* 23:2552-2562.
- Stubbs, M., Harris, M., Solomonow, M., Zhou, B., Lu, Y. and Baratta, R. V. (1998). Ligamento-muscular protective reflex in the lumbar spine of the feline. *J Electromyogr Kinesiol* 8:197-204.
- Stulen, F. B. and DeLuca, C. J. (1981). Frequency parameters of the myoelectric signal as a measure of muscle conduction velocity. *IEEE Trans Biomed Eng* 28:515-523.
- van Dieen, J. H., Selen, L. P. and Cholewicki, J. (2003). Trunk muscle activation in low-back pain patients, an analysis of the literature. *J Electromyogr Kinesiol* 13:333-351.
- Xu, Y., Bach, E. and Orhede, E. (1997). Work environment and low back pain: the influence of occupational activities. *Occup Environ Med* 54:741-745.
- Youssef, J, Davidson, B., Zhou, B.H., Lu, Y., Patel, V., and Solomonow, M. (2008). Neuromuscular neutral zones response to static lumbar flexion: muscular stability compensator. *Clin Biomech (Bristol, Avon)* submitted.